Deutsches Zentrum
für Luft- und Raumfahrt
German Aerospace Center

Institut für
Automatisierungstechnik

Master Thesis

Modelling and Economic Evaluation of Energy Management Storage Systems in Offshore Wind Farms Using Lithium Batteries

Kuete Kouam Georges Anicet

October 20, 2025

Thesis Number: MT2530

Tutor:
Dr. Arto Niemi
Dr.-Ing. Sergio Felipe Contreras Paredes

First Examiner:
Prof. Dr.-Ing. Johanna Myrzik

Second Examiner:
Dr.-Ing. Holger Groke

Universität
Bremen

Master Thesis

Modelling and Economic Evaluation of Energy Management Storage Systems in Offshore Wind Farms Using Lithium Batteries

Background: Renewable energy production capacity is increasing in Germany and in the North Sea region. This region has a high potential for offshore wind farms. The North Sea is relative shallow, which allows using turbines with fixed foundations. Therefore, all countries in this region have ambitious plans to build new offshore wind farms. Intermittent nature of renewable energy generation is a challenge concerning the increase of production capacity. The potential to produce the energy is not linked to actual demand. When the production potential is the best, the market price can plummet, as there might not be demand for energy. Therefore, there is a case for storing renewable energy when the market prices are low to sell it with a higher price later.

Objectives: This thesis will address the economical feasibility of energy storages for offshore wind farms considering common lithium-ion batteries.

[Obj1] Define a system model where an energy storage system can be located in an offshore or an onshore location considering a cluster of wind farms connected with a high voltage DC cable to the shore. For example, the case could be build considering the existing cluster consisting of Veja Mate, Deutsche Bucht, and Albatros wind farms that are connected through BorWin Beta platform and BorWin2 cable.

[Obj2] Define an energy management system to define rules when the electricity should be stored and when it should be provided to the grid. Energy management system should consider following inputs:

1. Current / momentary electricity production capacity of the cluster (based on the weather);
2. Weather forecast, defining near future production capacity of the cluster (reasonable accurate weather forecast can be expected for up to 2 or 3 days);
3. Current price of the electricity;
4. Price forecast for electricity (Can be expected to be reasonable accurate also for to 2 or 3 days); and
5. Current amount of stored energy.

[Obj3] Calculate the amount of revenue that could be created annually by the energy storage. Compare this potential revenue to rough lifecycle cost calculation. Can the energy storage be profitable considering the historical electricity market prices?

Material:

1. Historical weather data: https://www.ecmwf.int/en/forecasts/dataset/ecmwf-reanalysis-v5
2. Historical electricity prices from German market for industrial customers: SMARD | Download market data *(We also considered households, but the variability of prices seems to be higher in the electricity market for industrial customers)*
3. Simulink model: DLR-MI has an existing simple model combining weather data with a power curve from a wind turbine that can be used as a starting point for a new model: Part 10 Cybersecurity and Functional Safety in Hazardous System & Research Challenges Concerning Sustainability, Safety and Security – European Safety and Reliability Conference ESREL 2024 (pp. 39-48)

Dr. Arto Niemi, arto.niemi@dlr.de

Declaration of honour

I hereby confirm on my honor that I personally prepared the present academic work and carried out myself the activities directly involved with it. I also confirm that I have used no resources other than those declared. All formulations and concepts adopted literally or in their essential content from printed, unprinted or Internet sources have been cited according to the rules for academic work and identified by means of footnotes or other precise indications of source.

The support provided during the work, including significant assistance from my supervisor has been indicated in full.

The academic work has not been submitted to any other examination authority. The work is submitted in printed and electronic form. I confirm that the content of the digital version is completely identical to that of the printed version.

Date: _____ Signature: _____

Declaration of publication

- ☐ I hereby agree, that my thesis will be available for third party review in purpose of academic research.
- ☐ I hereby agree, that my thesis will be available after 30 years (§7 Abs. 2 BremArchivG) in the university archive for third party review in purpose of academic research.
- ☐ I hereby do *not* agree, that my thesis will be available for third party review in purpose of academic research.

Datum: _____ Unterschrift: _____

Abstract

Germany's rapid expansion of offshore wind energy necessitates solutions to manage production variability and capitalize on market opportunities. This thesis investigates the economic viability of lithium-ion battery energy storage systems (BESS) integrated with offshore wind farms for energy arbitrage in the German day-ahead market (DAM), exploiting price volatility to maximize revenue. A system model evaluates onshore and offshore BESS placement, focusing on BESS-related investment costs, using a case study of wind farm clusters connected to the BorWin2 platform in the German North Sea. An energy management system, employing mixed-integer linear programming and model predictive control, optimizes charging and discharging based on wind power production, weather forecasts, electricity prices, and storage levels, while incorporating realistic battery degradation to balance revenue and longevity. Simulations using historical data from 2021 to 2024 assess a 125 MW BESS with energy capacities ranging from 125 to 625 MWh. The optimal configuration was identified as an onshore 5-hour (625 MWh) storage system under 2023 day-ahead market price levels, which demonstrated marginal economic viability with an internal rate of return of 8.10%. Under a 7% discount rate assumption, this corresponds to a net present value of 11.29 M€ and a payback time of 16.8 years, emphasizing the need for patient capital and supportive financing. Offshore configurations were found economically unfeasible due to elevated installation and maintenance costs. Sensitivity analysis indicates that capital expenditure and market price volatility are key drivers, while Germany's continued renewable expansion may influence electricity prices and, consequently, arbitrage opportunities. Exploring additional revenue streams, such as intraday markets or ancillary services, could further enhance profitability or mitigate risks.

Keywords: Battery energy storage system, energy management system, energy arbitrage, MILP optimization, lithium-ion battery, economic evaluation

Kurzfassung

Der schnelle Ausbau der Offshore-Windenergie in Deutschland erfordert Lösungen, um die Produktionsschwankungen zu bewältigen und Marktchancen zu nutzen. Diese Arbeit untersucht die wirtschaftliche Tragfähigkeit von Lithium-Ionen-Batteriespeichersystemen (BESS), die in Offshore-Windparks integriert sind, zur Energiearbitrage auf dem deutschen Day-Ahead-Markt (DAM), um Preisvolatilitäten zur Maximierung der Erlöse auszunutzen. Ein Systemmodell bewertet die Platzierung von BESS an Land und auf See, wobei der Schwerpunkt auf den BESS-bezogenen Investitionskosten liegt, anhand einer Fallstudie von Windpark-Clustern, die mit der BorWin2-Plattform in der deutschen Nordsee verbunden sind. Ein Energiemanagementsystem, das gemischt-ganzzahlige lineare Programmierung und modellprädiktive Steuerung einsetzt, optimiert das Laden und Entladen auf der Grundlage der Windenergieproduktion, der Wettervorhersagen, der Strompreise und der Speicherfüllstände und berücksichtigt dabei eine realistische Degradation der Batterien, um ein Gleichgewicht zwischen Erträgen und Langlebigkeit herzustellen. Simulationen mit historischen Daten von 2021 bis 2024 bewerten ein 125 MW BESS mit Energiekapazitäten von 125 bis 625 MWh. Die optimale Konfiguration wurde als ein landgestütztes Speichersystem mit einer Speicherdauer von 5 Stunden (625 MWh) unter den Day-Ahead-Marktpreisniveaus des Jahres 2023 identifiziert, das mit einer internen Verzinsung von 8,10% eine grenzwertige wirtschaftliche Rentabilität aufwies. Bei einem angenommenen Diskontsatz von 7% entspricht dies einem Kapitalwert von 11,29 Mio. € und einer Amortisationszeit von 16,8 Jahren, was die Notwendigkeit von geduldigem Kapital und einer unterstützenden Finanzierung unterstreicht. Offshore-Konfigurationen erwiesen sich aufgrund der erhöhten Installations- und Wartungskosten als wirtschaftlich nicht tragfähig. Die Sensitivitätsanalyse zeigt, dass die Investitionsausgaben und die Marktpreisvolatilität die Haupttreiber der wirtschaftlichen Ergebnisse sind, während der fortgesetzte Ausbau der erneuerbaren Energien in Deutschland die Strompreise und damit auch die Arbitragemöglichkeiten beeinflussen könnte. Die Erschließung zusätzlicher Erlösquellen, etwa durch Intraday-Märkte oder Systemdienstleistungen, könnte die Rentabilität weiter steigern oder Risiken abmildern.

Schlüsselwörter: Batteriespeichersystem, Energiemanagementsystem, Energiearbitrage, MILP-Optimierung, Lithium-Ionen-Batterie, Wirtschaftlichkeitsbewertung

Acknowledgements

I extend my heartfelt thanks to everyone who has supported me throughout the completion of this master's thesis.

First, I am deeply grateful to my company tutor, Dr. Arto Niemi, for his invaluable guidance and encouragement. His expertise and mentorship have been instrumental, far exceeding the role of a tutor. Similarly, I sincerely thank my academic tutor, Dr. Sergio Felipe Contreras Paredes, for his insightful advice and support, which have greatly shaped this work. Together, they have been true mentors, inspiring me every step of the way.

I also express my sincere gratitude to my supervisors, Prof. Johanna Myrzik and Dr. Holger Groke, for kindly agreeing to oversee my research. Their support and willingness to guide me throughout this project have been greatly appreciated and instrumental in the successful completion of this thesis.

My thanks go to Dr. Bartosz Skobiej, my supervisor at DLR, for his constructive suggestions and engaging exchanges, which aided the development of this thesis. I am also grateful to Dr.-hab. Frank Sill Torres, the director of DLR Bremerhaven, for fostering a supportive environment that greatly facilitated the completion of this thesis.

I am grateful for the OASIS project, which provided the funding essential to making this thesis possible. The OASIS project is co-financed by the European Union under the European Regional Development Fund (ERDF) within the Interreg North Sea Region Programme 2021-2027.

To my friends Ornella and Helen, thank you for your constant encouragement and valuable advice, which kept me motivated. Finally, to my partner Debora, your steady support has given me strength throughout this journey.

Thank you all for making this thesis possible.

Contents

List of Symbols

Symbol	Term	Unit SI
c^{aging}	Degradation cost per unit of lost or battery capacity	€/MWh
Cal_{deg}	Calendar degradation of the battery energy storage system (BESS)	–
Cyc_{deg}	Cycling degradation of the BESS as a function of equivalent full cycles	–
E_{nom}	Nominal BESS capacity	MWh
FEC^{EOL}	Total equivalent full cycles of the BESS at end of life (EOL)	–
$P^{\text{ch}}_{\text{BESS}}$	Charging power of the BESS	MW
$P^{\text{dh}}_{\text{BESS}}$	Power discharged by the BESS to the grid	MW
$P^{\text{loss}}_{\text{wind}}$	Wind power losses due to curtailment	MW
$P^{\text{gen}}_{\text{wind}}$	Net wind power generated from the offshore wind farm	MW
δ_{ch}	Binary variable indicating BESS charging mode	–
δ_{dh}	Binary variable indicating BESS discharging mode	–
η_{ch}	Charging efficiency of the BESS	–
η_{dh}	Discharging efficiency of the BESS	–

List of Abbreviations

Abbreviation	Definition
AC	Alternating current
BESS	Battery energy storage system
CAPEX	Capital expenditure
DAM	Day-ahead market
DC	Direct current
EMS	Energy management system
EOL	End of life
ESS	Energy storage system
EU	European Union
IRR	Internal rate of return
kWh	Kilowatt hour
MILP	Mixed-integer linear programming
MPC	Model predictive control
MW	Megawatt
MWh	Megawatt hour
NPV	Net present value
OPEX	Operational expenditure
OWT	Offshore wind turbine
PBT	Payback time
RTE	Round-trip efficiency
SOC	State of charge
WT	Wind turbine

Chapter 1

Introduction

Recent years have seen considerable progress in Europe's renewable energy generation. In order to transition towards a competitive low-carbon economy, the European Union (EU) aims at reducing greenhouse gas emissions by 80-95% by 2050 compared to 1990 [1]. Germany, in particular, has made significant progress in increasing its renewable energy generation capacity, in line with the EU's strategic directives. In 2024, Germany's total electricity production amounted to about 515 billion kWh, of which approximately 57% was derived from renewable energy sources. Within this renewable share, wind power contributed the largest portion at 28%, followed by photovoltaic energy at 15% [2], as illustrated in Figure 1.1.

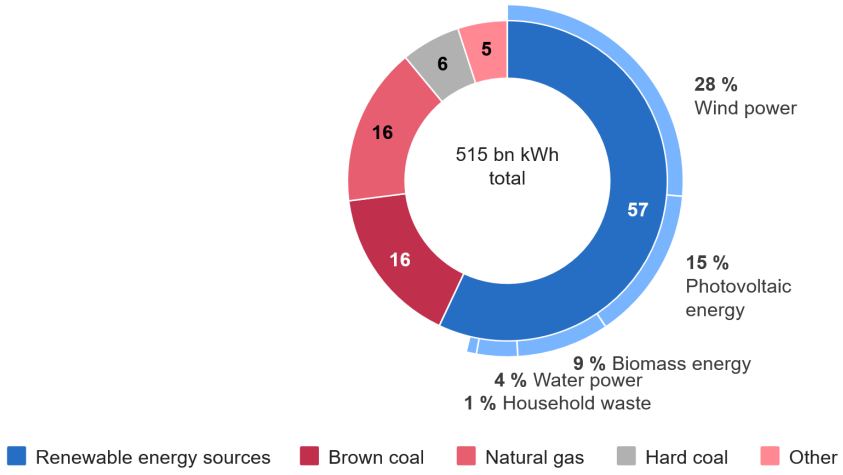

Figure 1.1: Gross Electricity Production in Germany as of 2024 [2]

Germany has set itself the target of increasing its gross green electricity production to a minimum of 80% of its overall electricity production by 2050 [3]. In addition, it has committed to ceasing all coal-fired power generation by 2038 [3]. To support this transition, a strong policy framework for renewable energy production is essential. In order to facilitate the ongoing renewable energy transition, there has been rapid development of offshore wind power in the European region. As of the latest figures, the total capacity of offshore wind turbines (OWT) in Germany is estimated to be approximately 9.2 GW at the end of 2024 [4]. Higher rates of expansion are anticipated by the end of the decade. The Federal Government set targets of increasing the installed offshore wind turbine capacity connected to the grid to a minimum of

30 GW by the year 2030 and at least 70 GW by 2045 [5, 6]. These offshore wind turbines are primarily located in the North Sea region, within Germany's exclusive economic zone, leveraging the strong and consistent wind resources available in this area [4].

The intermittent and seasonal nature of renewable energy generation necessitate the development of efficient energy storage solutions to mitigate imbalance between demand and supply [7]. Energy storage systems have been crucial in enhancing grid stability, resilience and flexibility by contributing to frequency regulation, peak load management, voltage control, and black start capability [7]. Over the past decades, a variety of electricity storage systems have been developed, with battery energy storage systems (BESS), particularly lithium-ion batteries, exhibiting high potential for grid-level energy storage applications due to their high energy density, high efficiency and long cycle life [8]. Despite their potential, the substantial costs of lithium-ion battery energy storage systems limit their broader implementation, thereby driving research into their economic feasibility for specific energy storage applications [7, 8]. In 2024, Germany saw a substantial increase in its installed battery capacity, rising from 8.6 GW to 12.1 GW [9]. Its storage capacity also grew from 12.7 GWh to 17.7 GWh [9], indicating an increase of 5 GWh of total energy reserve.

1.1 Research Motivation

Offshore wind energy is a cornerstone of Germany's renewable energy transition, offering significant economic potential due to its reliable wind resources [2]. However, a significant challenge persists: the inherent mismatch between wind power generation and electricity demand. Wind farms often produce more electricity than the market needs, resulting in wasted energy or curtailed production. Conversely, during periods of high demand and high prices, wind generation may be insufficient, resulting in missed revenue opportunities. Therefore, storage technologies could be adopted to ensure an appropriate balance between energy demand and supply [10].

This is where a battery energy storage system (BESS) become crucial. The core economic benefit of BESS lies in energy arbitrage [11]. This strategy directly addresses the temporal mismatch between wind power production and grid demand, transforming what would otherwise be lost energy into a significant revenue stream. Energy arbitrage is a key factor in ensuring the profitability of energy storage systems [11]. Lithium-ion BESS, in particular, with their high power density, rapid recharging time, and extended storage life, offer a promising avenue for strategic energy arbitrage within Germany's day-ahead market (DAM) [12].

While the initial capital investment for BESS technology is substantial [10, 11], the potential for lithium-ion BESS to significantly boost the economic viability of offshore wind farms through arbitrage is a powerful motivator for this research. This study will delve into the technical and economic feasibility of integrating BESS with offshore wind farms, comparing onshore and offshore deployment scenarios to provide critical insights for stakeholders navigating Germany's evolving renewable energy landscape.

1.2 Research objectives

The main objective of this thesis is to evaluate the economic feasibility of integrating lithium-ion BESS with offshore wind farms within the context of energy arbitrage in Germany's day-ahead market (DAM). To manage this integration and maximize revenue, an energy management system (EMS) will be developed. Furthermore, the analysis will be grounded in a case study of an offshore wind farm cluster.

The specific objectives are:

- Develop and simulate offshore wind power generation. This model will use historical wind speed data and turbine-specific power curves to determine power output of an offshore wind farm. The case study for this analysis will be the wind farm cluster connected to the BorWin Beta platform in the German North Sea.
- Design and implement an energy management system (EMS) optimization framework to maximize revenue through energy arbitrage in the German day-ahead market using a lithium-ion BESS specifications. The framework will employ mixed-integer linear programming (MILP) and model predictive control (MPC) optimization techniques, to determine optimal BESS charging and discharging schedules.
- Assess the economic viability of BESS-integrated offshore wind farms using a financial evaluation methodology.
- Conduct sensitivity analysis on relevant parameters including day-ahead market price volatility and BESS system parameters.

By addressing these objectives, this research aims to offer insights and potential guidance for policymakers, investors, and grid operators. This will help inform the effective and economically viable integration of large-scale offshore wind with lithium-ion BESSs into the German electricity grid, supporting the transition to a more sustainable, reliable, and efficient energy landscape.

1.3 Scope of the thesis

To effectively address the research objectives of this thesis, it is necessary to delimit its scope. The study is confined to the following key aspects:

- **Technology focus:** Lithium-ion BESS are exclusively considered, chosen for their high energy density, efficiency, rapid response times and suitability for grid-scale applications [13].
- **Integration strategy:** The study specifically examines the viability of integrating a new BESS system into an existing offshore wind farm, where investment costs relate to the BESS only.

- **Market focus:** The scope is limited to energy arbitrage within the German day-ahead market (DAM).
- **BESS energy flow:** To minimize reliance on external energy inputs and optimize renewable energy use, the BESS is designed for exclusive charging by the wind farm's generation, without drawing energy from the grid.

1.4 Thesis structure

To present the research conducted in this thesis, it is organized into six chapters.

Chapter 1 provides an overview of the energy transition in the German market, emphasizing the role of renewable energy and storage in addressing climate change challenges. It outlines the research motivation, objectives, and scope, highlighting the potential of BESS to enhance the economic performance of offshore wind farms.

Chapter 2 establishes the foundational research and materials addressing the thesis objectives, covering wind energy systems, the German electricity market, optimization techniques, and battery energy storage systems (BESS). It focuses on lithium-ion BESS, detailing their electrochemical properties, components, key characteristics, and their degradation.

Chapter 3 presents the research methodology, detailing the technical framework for wind power generation modeling and the mixed-integer linear programming (MILP) model for energy arbitrage, including its operational constraints and battery degradation considerations. It also describes the economic evaluation framework and introduces the case study.

Chapter 4 presents the simulation results, showing the influence of key parameters on financial metrics such as the net present value (NPV), the internal rate of return (IRR), and the payback time (PBT). The results specifically present the outcomes of wind power generation, energy arbitrage operations, economic performance, BESS configurations, and sensitivity analysis.

Chapter 5 discusses the results of the study and describes the conditions under which BESS integration achieves economic viability. It also examines the effects of parameter variations revealed by the sensitivity analysis and addresses the study's assumptions and limitations.

Chapter 6 summarizes the key findings, underscoring the marginal economic feasibility of BESS-integrated offshore wind farms under current market conditions and discussing the scope for future research to enhance project viability.

Chapter 2

Literature review

This chapter provides an overview of energy storage systems (ESS) for offshore wind farms, focusing on lithium-ion battery energy storage systems (BESS). It explores wind turbine technology, ESS types, and the key characteristics and degradation mechanisms of BESS. The chapter also outlines the structure of the German electricity market to establish the economic context. Finally, optimization techniques and simulation frameworks are reviewed to support the modeling presented in this thesis.

2.1 Wind energy systems

2.1.1 Wind turbine technology

Wind turbines (WTs) are systems that convert the kinetic energy from wind into mechanical energy, which is then converted into electricity [14]. As illustrated by Figure 2.1, the blades are mounted on the rotor hub, which is connected to the gearbox via the main shaft. The nacelle accommodates the gearbox and generator, while the tower supports the entire structure. WT controls adjust the pitch and yaw angles of the blades to control power production. Blades can be mounted on either a vertical or horizontal axis. Those mounted on a vertical axis are called vertical axis WTs (VAWT), while those mounted on a horizontal axis are called horizontal axis WTs (HAWT). HAWTs are mostly used nowadays due to their higher power efficiencies and capacity factors [15, 16]. Wind turbines are also classified based on their installation environment. Onshore wind turbines are deployed on land, whereas offshore wind turbines (OWTs) are installed in water bodies.

Working principle

Wind turbines harness kinetic energy from the wind and convert it into electrical energy. When wind passes over the turbine's blades, the difference in air pressure on either sides of the blades generates a lift force, causing them to rotate. This rotational mechanical energy is then transmitted through a drivetrain (which may include a gearbox for geared turbines) to a generator, which converts it into electricity. The amount of energy generated depends on the wind speed, as well as the technical specifications of the wind turbine [15, 14].

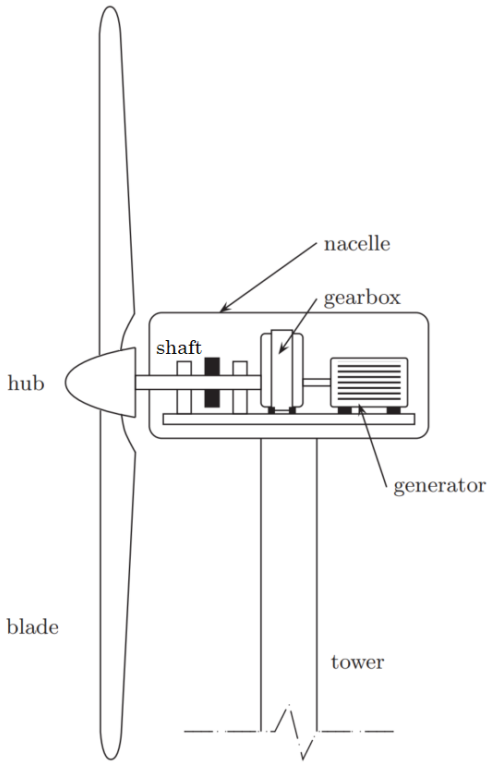

Figure 2.1: Simplified structure of a WT [17]

The theoretical power (P_{wind}) harnessed by the wind turbine is given by equation 2.1 [18]:

$$P_{wind} = \frac{1}{2}\rho A v^3 \tag{2.1}$$

where:

- ρ is the air density (kg/m^3)
- A is the swept area of the turbine blades (m^2)
- v is the wind velocity (m/s)

In practice, wind turbines can only capture a fraction of this theoretical power due to fundamental physical and engineering limitations. The actual electrical output is given by equation 2.2 [18]:

$$P_{electrical} = \eta C_p P_{wind} \tag{2.2}$$

where:

- η is the turbine's overall efficiency
- C_p is the power coefficient

The overall efficiency η is a composite of multiple component efficiencies, specifically gearbox efficiency (η_{gear}), generator efficiency (η_{gen}), and electrical efficiency (η_{elec}), as shown in equation 2.3 [14].

$$\eta = \eta_{\text{gear}}\eta_{\text{gen}}\eta_{\text{elec}} \tag{2.3}$$

The generator efficiency reflects losses from electrical and mechanical sources within the wind turbine, including those due to copper, iron, friction, and from other miscellaneous sources. The electrical efficiency accounts for combined power losses in the converter, control systems, switches, and cabling [14].
The power coefficient (C_p) quantifies the theoretical mechanical power a turbine rotor can extract from the wind. Combined with the overall efficiency (η), these factors determine the turbine's actual power generation. C_p itself is influenced by aerodynamic operating conditions [18]. The theoretical maximum C_p, also known as the Betz limit, is 0.5926 [18]. While this represents the total power available, the actual power generated by a wind turbine is described by its power curve, a crucial characteristic provided by the turbine manufacturer, illustrating the power output at different wind speeds [18].

Power curve

The power curve of a wind turbine (WT) defines the relationship between wind speed and the generated power. The operating limits of the turbine are defined by the cut-in and cut-out speeds. There is little or no power output at wind speeds below the cut-in speed threshold. The rated speed is the speed at which the power output reaches its maximum value; any further increase in speed will not increase the power output [16, 18]. The control system of the WT inhibits power production when the wind speed reaches a value that could potentially damage the WT. This value is the cut-out speed [14, 15]. The design characteristics of a wind turbine and the weather conditions at its installation site also influence the shape of its power curve [15]. Figure 2.2 shows a typical power curve of a WT [16].

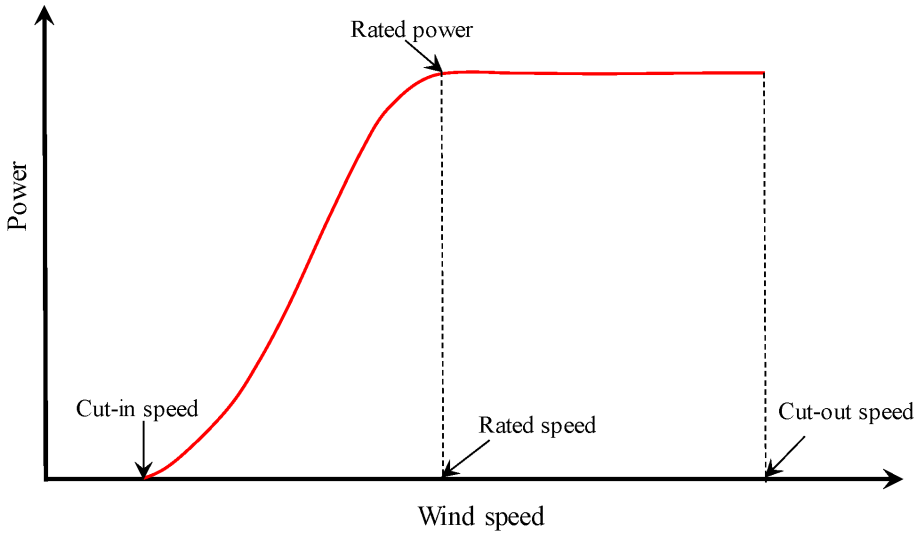

Figure 2.2: Typical power curve of a WT [16]

2.1.2 Offshore wind energy systems

Overview

Offshore wind energy has emerged as a crucial component of the global renewable energy landscape, offering significant potential for large-scale power generation while simultaneously enhancing security of supply and system quality through its reliability [19]. Offshore wind farms typically consist of multiple wind turbines which are located in water bodies. A distinguishing feature of modern large-scale offshore wind projects is the utilization of offshore converter platform [20]. These platforms play a crucial role in reducing electrical losses by increasing voltage levels before transmission [20].

For instance, in the North Sea off the coast of Germany, power from offshore wind farms is transmitted to the BorWin2 offshore converter platform via 155-kV three-phase alternating current (AC) cables, where the AC current is converted to direct current (DC) [21]. From the offshore platform, power is transmitted via submarine and underground high voltage (HV) cables to the land station where it is converted back into AC and fed into the grid as shown in Figure 2.3 [22]. The choice between high voltage alternating current (HVAC) and high voltage direct current (HVDC) cables is primarily influenced by the transmission distance. Although HVACs do not require additional converters at the shore, their high capacitance significantly reduces power ratings over longer distances, making them ideal for short-distance power transmission. Conversely, HVDC cables are preferred for long-distance power transmission due to their significantly lower transmission losses [20].

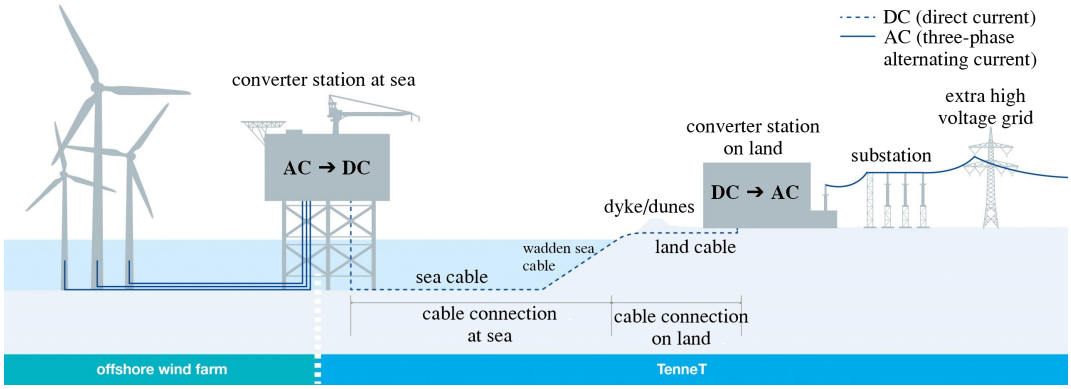

Figure 2.3: Overview of offshore wind system configuration [22]

Offshore wind farms generally achieve higher energy yields than their onshore counterparts, attributable to the stronger and more consistent wind resources prevalent in deeper marine environments [23]. However, this benefit is offset by the high initial investment required for offshore projects, as well as challenges related to maintenance under harsh marine conditions, logistical constraints, and limited site availability due to conflicts with maritime activities and conservation areas [24].

Current state of offshore wind development

In 2024, global offshore wind power saw an increase of 11 GW in new capacity, bringing the total operational capacity worldwide to approximately 78.5 GW [25]. Europe alone contributed approximately 2.6 GW of this capacity, bringing its total operational offshore wind power capacity to 21 GW [26]. Germany contributed substantially to Europe's offshore wind growth. As of June 2024, it had connected 1,602 offshore wind turbines to the grid, primarily in the North and Baltic Seas, accumulating an installed capacity of approximately 8.9 GW [6]. In 2024, Germany further increased its offshore capacity by integrating two wind farms into the grid: the Baltic Eagle (477 MW) and the Gode Wind 3 (253 MW), contributing a combined capacity of 730 MW and raising the total offshore capacity to 9.2 GW [4, 6].

Offshore wind farms in Germany

The majority of offshore wind farms in Germany are located off the German coast, at a minimum distance of 40 kilometers from the shore and in water depths of at least 20 meters [6]. German offshore wind projects are located in the North Sea and the Baltic Sea, with the North Sea being a major contributor [6]. Figure 2.4 shows the distribution of offshore wind farms in Germany across the North Sea and Baltic Sea as of mid-2024, while Table 2.1 summarizes key data for selected offshore wind farms in these regions during the same period.

Table 2.1: Selected offshore wind projects in Germany as of mid-2024

Region	Project	Capacity (MW)	Status	Source
North Sea	Borkum Riffgrund 1, 2	312, 448	Operational	[6, 27]
	Borkum Riffgrund 3	913	Not yet operational	
	Gode Wind 1, 2, 3	330, 252, 253	Operational	
	Kaskasi	342	Operational	[6]
	Nordsee Ost	295		
	Nordsee One	332		
	Deutsche Bucht	252		
	Veja Mate	402		
	Albatros	112		
Baltic Sea	Baltic Eagle	476	Operational	[6]
	Arkona	378		
	EnBW Baltic 1, 2	48, 302		
	Wikinger	366		

2.2 Energy storage system (ESS)

An energy storage system (ESS) is designed to capture energy, usually electricity, convert it into a storable form, and then release it back as electricity when required [28]. The growing penetration of variable renewable energy sources like wind and solar necessitates ESS for modern power grids to address their intermittency [10]. These

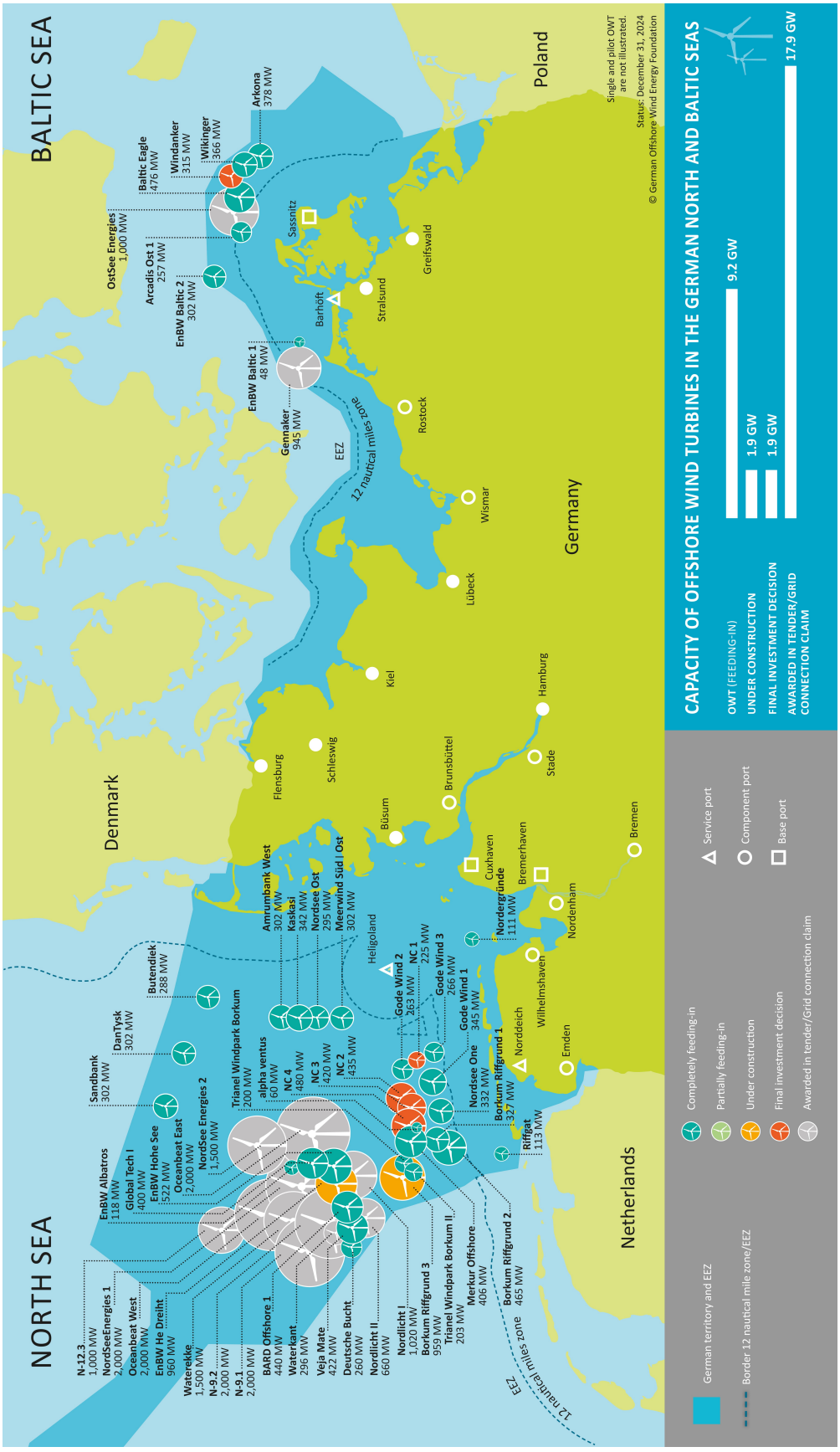

Figure 2.4: Offshore wind power facilities near Germany's North Sea and Baltic Sea shores as of mid-2024 [6]

systems are crucial for maintaining grid stability by ensuring a continuous and uninterrupted power supply, especially through services like frequency regulation or load balancing [12]. Energy storage systems typically operate through three key stages; charging, storing, and discharging [12].

Energy storage systems (ESS) are broadly classified by the form of energy they store, distinguishing between their physical and chemical principles [28]. As shown in Figure 2.5, these technologies generally fall into the categories of mechanical, electrochemical, chemical, thermal and electrical storage [28]. Mechanical storage, such as pumped hydroelectric, compressed air, and flywheels, stores energy as potential or kinetic energy [10, 12, 29]. Thermal energy storage (TES) uses temperature changes or phase transitions, like sensible or latent heat storage [10]. Chemical energy storage (CES) stores energy in chemical bonds and releases it through chemical reactions [10]. Electrical storage, such as supercapacitors, uses electrostatic principles but is limited by high self-discharge rates [12, 29]. These technologies are not the focus of this study.

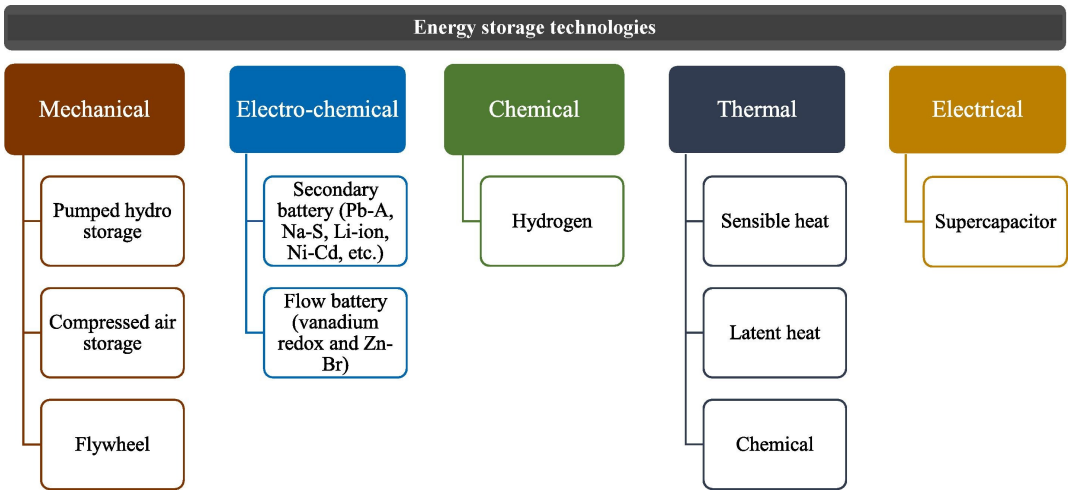

Figure 2.5: Energy storage system classification by storage medium [28]

2.2.1 Electrochemical energy storage

Electrochemical ESSs store and release energy through chemical reactions that result in the transfer of electrons in a battery [12]. This study focuses on lithium-ion batteries, though other technologies like lead-acid and flow batteries exist [28, 30].

Lithium-ion batteries

Lithium-ion batteries represent the dominant electrochemical ESS due to their high energy and power densities [28]. A typical lithium-ion cell fundamentally consists of a lithium metal oxide cathode, a carbon anode made of graphite, and a non-aqueous electrolyte containing a lithium salt [30]. These components, along with a separator and two current collectors, facilitate the movement and storage of lithium ions, while the separator prevents direct electron flow within the battery [20].

In the charging phase, lithium cations migrate from the cathode to the carbon anode, where they combine with electrons and deposit as lithium atoms between the carbon layers, as shown in Figure 2.6. Conversely, during discharge, these lithium atoms at the anode release electrons and lithium ions [30]. The ions then travel back through the electrolyte to the cathode, generating free electrons that can flow through an external circuit to power a device [30]. For instance, the overall reversible chemical reaction for a lithium-ion battery employing a lithium cobalt oxide ($LiCoO_2$) cathode can be represented as shown in equation 2.4 [30]:

$$LiC_6 + CoO_2 \rightleftharpoons C_6 + LiCoO_2 \tag{2.4}$$

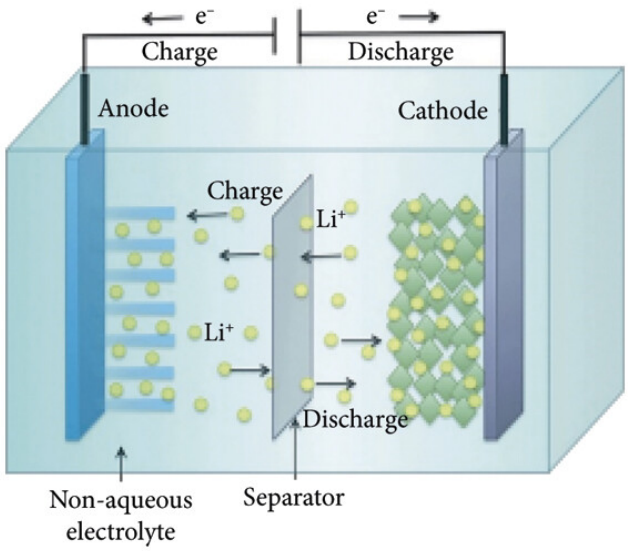

Figure 2.6: Charge and discharge operations in a Li-ion Cell [31]

The main types of lithium-ion batteries include lithium cobalt oxide (LCO), lithium nickel cobalt manganese oxide (NMC), lithium nickel cobalt aluminum oxide (NCA), lithium manganese oxide (LMO), lithium iron phosphate (LFP), and lithium titanate oxide (LTO) [32]. Lithium-ion technology offers superior performance metrics including high efficiency, high energy density, minimal self-discharge rates (1.5-2% monthly), and extended cycle life [30, 33]. Despite these benefits, the high capital cost remains the primary barrier to the widespread adoption of these batteries for large-scale applications [28, 33].

2.3 Battery energy storage system (BESS)

Battery energy storage systems are electrochemical ESSs that capture and store energy from various sources in rechargeable batteries for later use [34]. The primary components of a BESS as shown in Figure 2.7 include:

- **Battery system**: The foundation of any BESS lies in its battery system, comprising individual electrochemical cells that convert chemical energy into

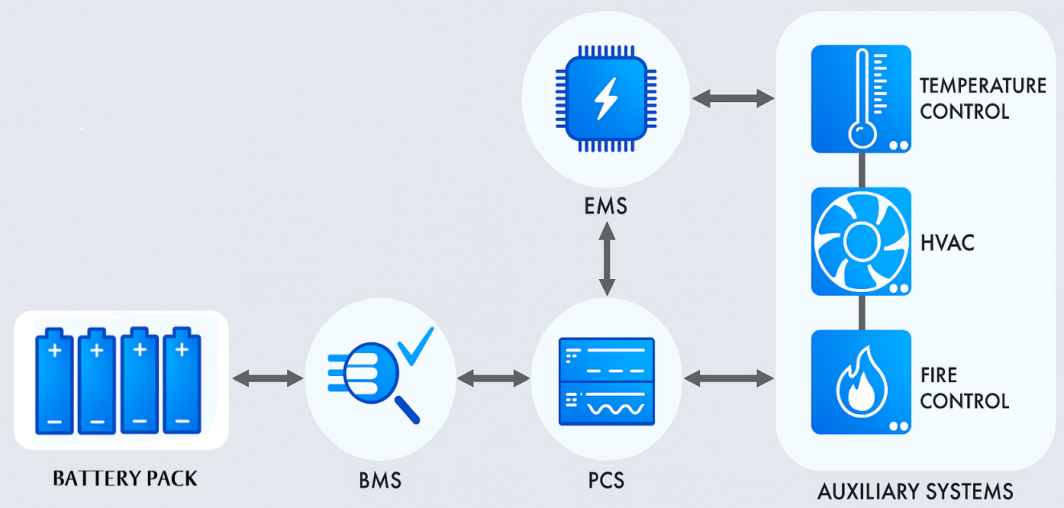

Figure 2.7: Functional blocks of a BESS [34]

electrical energy [34]. These cells are systematically organized into modules, which subsequently form larger battery packs [34]. The battery is made up of rechargeable secondary cells that are designed for repeated charging and discharging cycles [35].

- **Power Conversion System (PCS)**: The PCS is critical for converting direct current (DC) from the battery into alternating current (AC) suitable for grid or facility use [35]. Equipped with bidirectional inverters, it facilitates both charging and discharging while maintaining power quality [34].
- **Battery Management System (BMS)**: The BMS ensures operational safety by monitoring battery parameters such as state of charge (SOC) and state of health (SOH) [34]. It prevents overcharging, overheating, and other risks through real-time data analysis and external interfacing [35].
- **Energy Management System (EMS)**: The EMS oversees the entire BESS operation, coordinating the PCS and BMS to optimize energy flow. It determines optimal charging and discharging schedules to maximize efficiency and safety [34, 35].

Beyond these core components, BESS often incorporates safety systems such as fire suppression, smoke detection, and temperature control (cooling, heating, ventilation, and air conditioning) [34]. These auxiliary systems monitor operational conditions and respond to emergencies, ensuring safe and reliable operation [34].

BESS serve a variety of critical purposes across transmission and distribution grids. Primarily, they support ancillary services, with frequency containment reserve (FCR) being a dominant application. This helps stabilize the grid by rapidly balancing supply and demand. Furthermore, BESS are crucial for renewable energy integration, mitigating the variability of wind and solar generation [10]. In addition, BESS can be used for energy arbitrage [36], a concept that will be explored in this thesis in the context of offshore wind energy production.

As of January 2025, Germany's installed BESS capacity reached 2.2 GWh with a combined power of 1.7 GW. This represents a substantial increase from December 2022, when the total installed capacity was 863 MWh/787 MW, indicating a doubling of capacity in just two years and highlighting the rising interest in BESS [36].

2.3.1 BESS characteristics

Several characteristics define the performance and suitability of a BESS for specific applications:

- **Power and Energy Specifications:** The fundamental metrics of a BESS include both power and energy specifications. The Rated power capacity, measured in kilowatts (kW) or megawatts (MW), represents the maximum instantaneous electrical power a BESS can discharge or absorb [37]. It signifies the highest rate at which the battery can supply power from a fully charged state [37]. Complementing this, energy capacity defines the total amount of stored energy, expressed in kilowatt-hours (kWh) or megawatt-hours (MWh), representing the maximum energy that can be stored and subsequently delivered by the system [37]. The relationship between these parameters, also known as the energy-to-power ratio (E/P), determines the storage duration [38].

- **Storage duration and C-rate:** The storage duration and the C-rate are also important BESS parameters. The storage duration refers to the time required to fully discharge the system's usable energy capacity at its nominal power rating, starting from a fully charged state [37, 38, 39]. The C-rate quantifies the maximum charging or discharging rate relative to the battery's nominal energy capacity, indicating the speed at which the battery can be charged or discharged [39]. It is expressed as a multiple of the battery's nominal capacity [40]. For example, a C-rate of 1C corresponds to a full discharge in one hour, while a 2C rate implies a discharge time of 30 minutes.

  The C-rate is inversely related to the energy-to-power (E/P) ratio, which defines the maximum storage duration [38]. For instance, a 1 MW/2 MWh BESS has an E/P ratio of 2, corresponding to a storage duration of 2 hours and a C-rate of 0.5C. The relationship is expressed as shown in equation 2.5.

$$\text{Storage\_duration}_{\text{max}} = \text{E/P}_{\text{ratio}} = \frac{1}{\text{C-rate}} \tag{2.5}$$

  While the C-rate sets the maximum charge or discharge rate, a BESS can operate at lower rates. Through its controller module, the system can adjust the C-rate below its maximum, enabling flexible control of storage duration during charging and discharging [39]. This adaptability is valuable in energy management systems, allowing operators to tailor power flow to specific requirements.

- **Round-trip efficiency (RTE %):** This is the ratio of energy discharged from the BESS to the energy put into it during a full charge-discharge cycle, reflecting energy losses during power conversion [37, 38].

- **State of charge (SOC %):** The SOC indicates the percentage of the current energy level in the battery relative to its maximum capacity [37].
- **Depth of discharge (DoD %):** This refers to the percentage of the battery's total capacity that has been discharged [41].
- **State of health (SoH %):** The represents the ratio of the current usable energy capacity of the battery to its nominal energy capacity [38].
- **End of life (EOL %):** The EOL represents the SoH at which the BESS is considered no longer suitable for service and is retired [38]. In essence, it marks the point at which the battery's performance has deteriorated beyond an acceptable threshold [38].
- **Cycle life:** This represents the number of complete charge-discharge cycles a battery can undergo before its capacity drops below a predefined threshold (e.g., 80% of initial capacity) [38, 41].
- **Calendar life:** This represents the duration in years, until the battery reaches EOL without being operated on [38].

2.3.2 Battery degradation

Battery degradation represents a critical factor in assessing realistic performance expectations for a BESS. It represents a series of occurrences that diminish a battery's capacity to retain charge and produce power over time, primarily due to a gradual decrease in mobile lithium ions or charge carriers through intricate chemical and physical processes [42]. Battery degradation is broadly categorized into two main types:

- **Calendar degradation:** This type of degradation occurs irrespective of battery usage and is primarily a function of time [43]. It is sometimes referred to as self-degradation and represents the corrosion of internal materials unrelated to charging and discharging cycles [44]. The main influencing factors on calendar degradation are the average SOC and the temperature during operation [43, 45].
- **Cycle degradation:** Cycle degradation, in contrast, directly results from the operational use of the battery through charging and discharging processes [42, 43]. A complete battery charge cycle encompasses the full discharge of a battery to 0% followed by complete recharging to 100%, though partial cycles also contribute to overall degradation [42]. The cycle life refers to the total number of complete charge-discharge cycles a battery can endure before reaching its EOL [42]. Key factors influencing cycle degradation include the DOD for each cycle, the C-rate (charging/discharging rate), the temperature, and the average SOC during operation [10, 43, 45].

The mathematical formulation of battery degradation within battery energy storage system modelling poses significant challenges. However, its incorporation is imperative for a realistic assessment of battery performance. From an optimisation perspective, degradation effects can be integrated in two primary ways: by reducing

the cyclable capacity of the BESS during operation, or by defining a degradation penalty in the objective function to discourage excessive cycling [43]. In this study, both approaches will be employed. A simplified framework for cycle and calendar degradation, adapted from the literature and utilized in this work, is described in Section 3.3.2. For the optimization problem, cycle degradation will be introduced as a penalty in the objective function, to discourage excessive cycling and mitigate overall battery degradation

2.4 Electricity market in Germany

The German electricity market is a key component of the wider European energy market, with trading primarily occurring on the European Power Exchange (EPEX SPOT) [46, 47]. This market is organized into two main segments: the day-ahead market (DAM) and the intraday market (IDM) [46, 47]. These markets use a system of bidding zones to manage transactions and price formation [48].

2.4.1 Bidding zones

Within Europe, the electricity market is divided into multiple bidding zones [48]. A bidding zone is a geographical area where market participants can submit bids and offers, and a uniform, single price applies to all transactions within that zone, ignoring internal transmission capacity limitations [48]. Germany and Luxembourg together form a bidding zone known as the German-Luxembourgish zone [48]. This zonal pricing model promotes transparency and liquidity across a large region [48]. However, uniform pricing creates significant challenges, particularly in Germany where strong wind generation in northern regions must be transported to southern demand centers [48]. If the transmission lines become congested, costly redispatch actions are required by transmission system operators (TSOs) to stabilize the grid, with Germany incurring 3.1 billion € in redispatch costs in 2023 [48].

2.4.2 Day-ahead market (DAM)

The day-ahead market operates as a daily auction for the physical delivery of electricity on the following day [47, 49]. Trading on the EPEX SPOT for the German-Luxembourgish bidding zone closes daily at noon (12:00 CET) [46, 47]. In this auction, market participants submit bids and offers for hourly products that cover the 24 hours of the next day [46, 47, 49].

Available power plant capacities are sorted by their marginal costs, and the price is set by the marginal cost of the last and most expensive power plant needed to meet the demand for that hour [49]. Renewable energy sources like wind and solar, which have zero marginal costs, are offered at the lowest possible price, thus displacing conventional power plants and reducing the overall electricity price. This is known as the merit-order principle [49]. The intersection of the supply and demand curves in the auction sets the market clearing price (MCP), which applies to all accepted bids and offers for that specific hour [49].

2.4.3 Intraday market (IDM)

The intraday market (IDM) complements the day-ahead market by allowing continuous trading until shortly before delivery, enabling participants to adjust for forecast deviations and optimize schedules [50]. The necessity for intraday trading arises from inevitable mismatches between actual demand and supply that emerge after day-ahead market closure, as real-time conditions provide more accurate predictions than those available during initial planning [51].

Intraday trading in Germany is conducted on the EPEX SPOT exchange and begins with a quarter-hourly auction at 15:00 CET the day before delivery. This auction allows market participants to address imbalances between forecasted and actual supply or demand on a 15-minute resolution [50]. Following the auction, continuous trading of 15-minute, 30-minute, and hourly contracts is possible up to 5 minutes before delivery [46, 47].

Prices in the IDM are determined using a pay-as-bid mechanism, where each trade is settled at the offered price [50]. This creates characteristically wider price spreads compared to day-ahead markets, reflecting the increased uncertainty and urgency closer to delivery time [51]. These broader price spreads can provide opportunities for electricity arbitrage, though trading volumes remain relatively modest compared to day-ahead markets [51]. The intraday market's role is expected to become increasingly significant as variable renewable energy sources (VRES) continue to penetrate electricity systems, requiring more sophisticated balancing mechanisms [51].

2.5 Optimization techniques in battery energy storage systems

Integrating battery energy storage systems with wind energy production requires advanced optimization techniques to enhance cost efficiency and ensure reliable operation. Two widely used techniques are mixed-integer linear programming (MILP) and model predictive control (MPC) [52, 53].

2.5.1 Mixed-integer linear programming (MILP)

Mixed-integer linear programming (MILP) extends traditional linear programming by allowing both continuous and integer decision variables, making it suitable for BESS optimization tasks requiring discrete choices, such as switching between battery charging and discharging modes [54]. Studies such as [43, 55, 56, 57] have also employed MILP to evaluate the economic viability of BESS in grid energy storage applications, highlighting its utility in cost-benefit analysis and strategic planning. For instance, a MILP mathematical representation can be formulated as given by equation 2.6 [58]:

$$\begin{aligned} \text{minimize} \quad & c^T x + w^T y + d \\ \text{subject to} \quad & Gx + My \leq h \\ & Ax + Ny = b \\ & x \in \mathbb{R}; y \in \mathbb{Z} \end{aligned} \tag{2.6}$$

Here, x represents continuous variables, such as power flow or energy levels, while y denotes integer variables for binary decisions, like whether to charge or discharge the battery. The matrices G, A, M, N and vectors c, w, d, h, b define the problem constraints [58], such as power flow limits or battery state of charge boundaries.

2.5.2 Model predictive control (MPC)

MPC, also known as receding-horizon control, is an advanced control strategy that uses a system model to predict future behavior over a prediction horizon and optimize control actions while respecting constraints [58]. The fundamental principle involves solving finite-horizon optimization problems at each sampling instant, using the most recent state measurement or estimate as the initial condition for the prediction [59, 60]. The schematic of this operation is illustrated in Figure 2.8. The MPC methodology operates through a systematic process:

- **Prediction:** At each sampling time, a system model is used to forecast future system outputs over a prediction horizon [51, 60].
- **Optimization:** Optimal control signals are calculated by optimizing a cost function for the entire prediction horizon while respecting operational constraints [51, 53, 60].
- **Receding Horizon:** Only the first element of the optimal control sequence is implemented, following the receding-horizon principle [58, 59].
- **Repeat:** The horizon is then shifted forward by one time step, and the process is repeated with new measurements and updated information [60, 61].

The mathematical foundation of MPC centers on minimizing a cost function over a prediction horizon, as shown in equation 2.7 [53]:

$$\min_{u_k} \sum_{k=1}^{N} J(x, u) \tag{2.7}$$

where

- x represents the system states,
- u contains the control decisions,
- J represents the costs and penalties to be minimized.

This receding horizon approach allows the system to adapt to changes and disturbances in real time [59]. The ability of MPC to explicitly handle multiple and tight constraints makes it particularly well-suited for managing complex systems like battery storage, where constraints on state of charge and power limits are critical [51, 59].

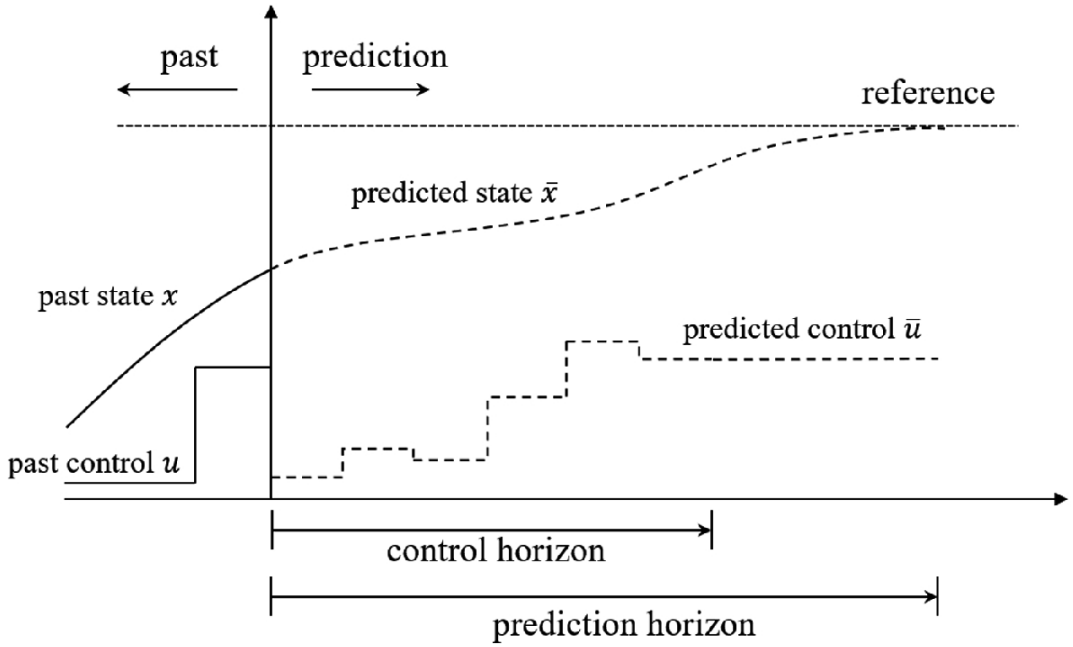

Figure 2.8: Schematic of MPC operation with prediction and control horizons [60]

2.5.3 Simulation framework and environment

The integration of MPC with a MILP model constitutes a robust framework for addressing complex, constrained optimisation problems in energy management [58], and this combination will serve as the foundation for the methodology employed in this thesis.

There are various frameworks and solvers available for implementing optimization problems.

- **Modeling Frameworks:** These are software packages that provide comprehensive interfaces for defining objective functions and constraints, solving complex optimization problems such as mixed-integer programming (MIP) and MILP models, and analyzing the results, while ensuring that all necessary constraints are properly incorporated. Some examples of these frameworks, all of which are open source, include *Pyomo* and *PuLP*, developed in the Python environment, and *JuMP*, developed in Julia [57, 62].
- **Solvers:** These are algorithms that find the optimal solution to the formulated optimization problem. Examples of open source solvers include *SCIP* (Solving constraint integer programs), *CBC* (COIN-OR branch and cut), and *GLPK* (GNU linear programming kit). Commercial solvers known for their superior performance on large-scale problems include *CPLEX*, *Gurobi*, and *COPT* (Cardinal optimizer). Many commercial solvers offer free academic licenses for theses and other academic projects, though a non-academic license can be quite expensive [62].

In this thesis, the MILP models were formulated using Python with the *Pyomo* library. This framework allowed for the precise definition of the objective function

and all necessary constraints. The *GLPK* solver was then used to find the optimal charge/discharge cycles and power dispatch schedules for the BESS over a defined time horizon for energy arbitrage.

Chapter 3

Research methodology

This chapter outlines the research methodology employed to evaluate the economic feasibility of integrating a lithium-ion BESS with offshore wind farms. The approach focuses on simulating energy production from the wind farm, optimizing charging and discharging strategies for the BESS to enable energy arbitrage, and conducting a comprehensive economic analysis.

3.1 System overview

The system topology presented in Figure 3.1 illustrates the complete energy management framework and data flow for the proposed configuration. The methodology simulates an integrated offshore wind farm system where wind data feeds into the offshore wind farm to generate variable power output. This wind power generation, along with real-time electricity prices, serves as input to the Energy Management System (EMS), which coordinates the optimal operation of the BESS. Energy can flow to the grid transformer from two sources: directly from the wind farm or from the BESS discharge. Wind speed data and electricity price information drive the decision-making process within the EMS.

3.2 Data collection

The following data were collected for the purpose of this thesis to serve as inputs for the system design:

3.2.1 Wind speed data

Wind speed data were extracted from the ERA5 reanalysis dataset provided by the Copernicus Climate Change Service (C3S) Climate Data Store (CDS) [63, 64]. For each offshore wind farm location, the lateral wind components u and v (in meters per second) at 100 meters above ground level were retrieved on a spatial grid with a resolution of 0.01° in latitude and longitude. The absolute wind speed was computed as the vector magnitude of these components as shown in equation 3.1 [63]:

$$speed_{100} = \sqrt{u^2 + v^2} \tag{3.1}$$

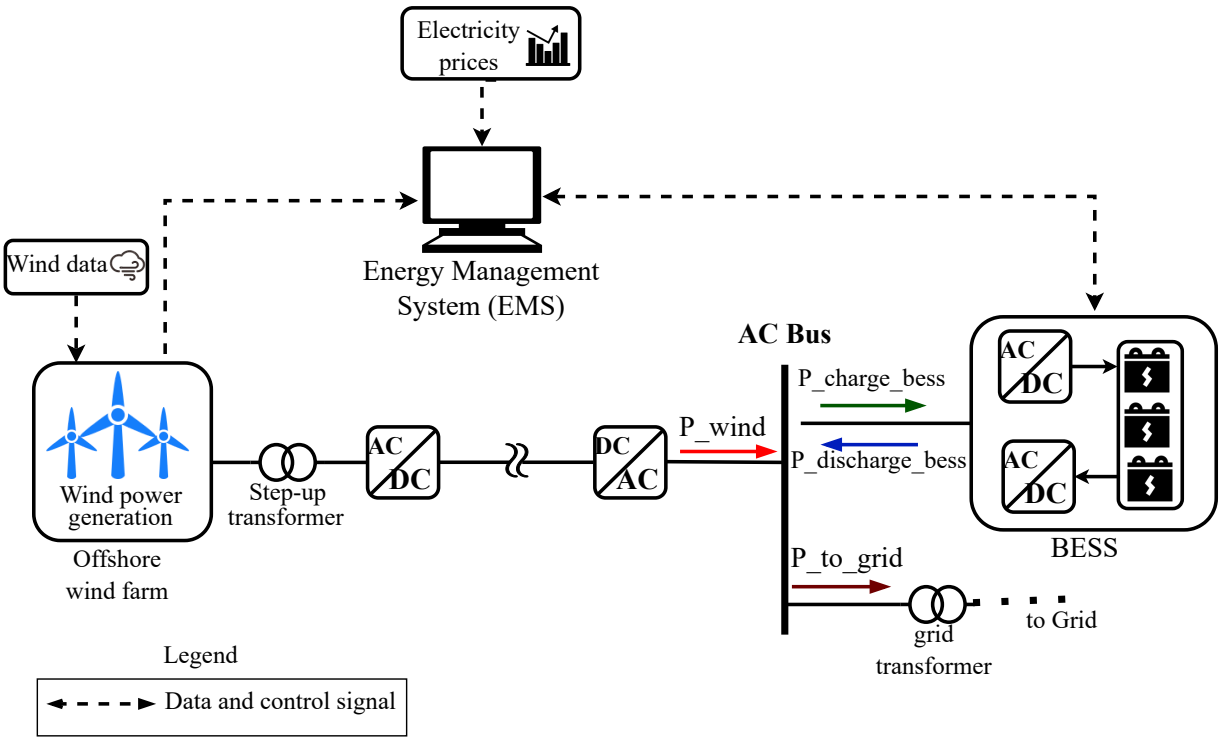

Figure 3.1: BESS system topology

To adjust wind speeds to turbine hub heights, a logarithmic wind profile was applied, which incorporates surface roughness parameters obtained from ERA5 [64]. The adjusted wind speed at hub height h_{hub} is calculated as given by equation 3.2 [63]:

$$speed_{hub} = speed_{100} \cdot \left[\frac{\log(100) - \log(z_0)}{\log(h_{hub}) - \log(z_0)} \right] \tag{3.2}$$

where z_0 represents the surface roughness.
For this thesis, wind speed data was collected with an hourly resolution for the period from 2021 to 2024.

3.2.2 DAM price data

DAM price data for the German-Luxembourg bidding region were obtained from the German electricity market platform SMARD [65]. The data were collected for the period of 2021 to 2024 with an hourly resolution to maintain consistency with the wind speed data.

In the year 2024, for instance, the minimum DAM electricity price was approximately -135 €/MWh, while the maximum reached about 936 €/MWh, with an average price of around 78 €/MWh. This price volatility, as illustrated in Figure 3.2, highlights potential arbitrage opportunities for BESS by exploiting fluctuations in market prices.

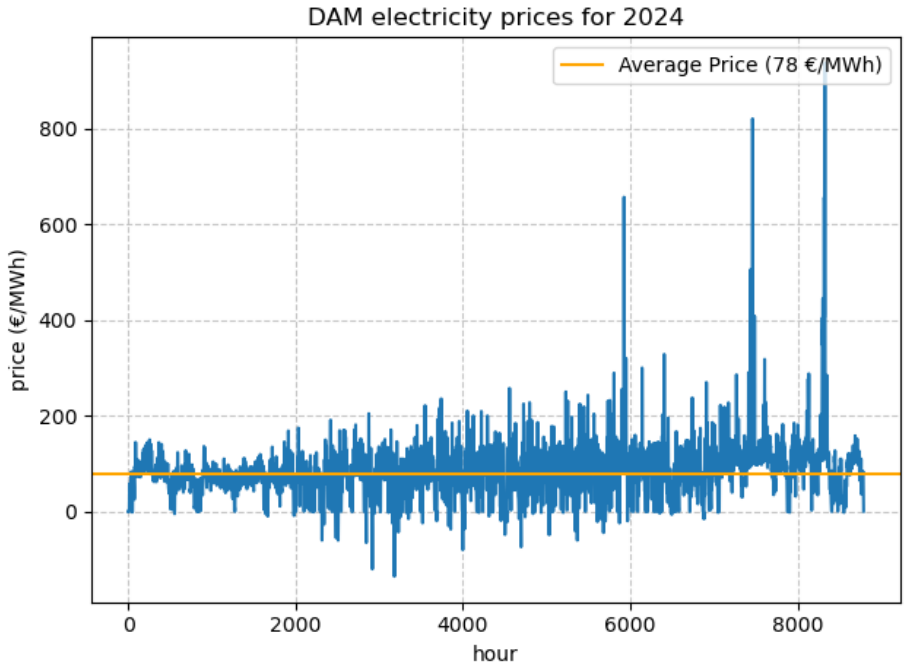

Figure 3.2: Sample DAM price data showing hourly price variations for the year 2024

3.2.3 Power curve data

Power curves were developed using turbine-specific characteristics for each offshore wind farm. Detailed data defining the relationship between wind speed and power output at known points were sourced from manufacturer specifications [66, 67], from which turbine-specific power curves were extracted. These curves were combined with the collected wind speed data to estimate power production for each turbine. The power curves are interpolated as described in Section 3.3.1, allowing for an approximate modeling of the overall power output of the offshore wind farm.

3.3 System Design

3.3.1 Wind power generation modeling

This section outlines the steps for approximating wind power generation as part of the thesis methodology. The approach integrates literature-based power curve modeling, wake effect considerations, and transmission losses to estimate the total power output of a wind farm.

Power curve approximation

Following the standard piecewise definition, the power $P_k(v)$ for a turbine type in wind farm k can be estimated following equation 3.3 [68, 69, 70],:

$$P_k(v) \approx \begin{cases} 0 & v < v_{\text{cut-in}},\ v > v_{\text{cut-out}}, \\ q(v) & v_{\text{cut-in}} \leq v \leq v_{\text{rated}}, \\ P_r & v_{\text{rated}} \leq v \leq v_{\text{cut-out}}, \end{cases} \tag{3.3}$$

where:

- $v_{\text{cut-in}}$, v_{rated}, and $v_{\text{cut-out}}$ represent the cut-in, rated, and cut-out wind speeds respectively
- P_r is the rated power output
- $q(v)$ is an interpolated function derived from wind speed-power data points for the turbine type in wind farm k.

The function $q(v)$ is approximated through cubic spline interpolation [68, 69]. This is implemented using the `scipy.interpolate.interp1d` function in Python to fit the curve between the known wind speed and power points.

Power losses

The power output derived from the turbine power curve is subject to various loss mechanisms that reduce the actual electricity generation. Wake effects, caused by kinetic energy extraction by upstream turbines, reduce downstream wind speeds and increase turbulence [27, 71]. Depending on the wind farm layout, turbine spacing, and site conditions, these effects can result in annual energy losses of approximately 10–40% [27]. In this thesis, a wake effect of 15% is assumed.

Additionally, turbine availability must be considered, as maintenance schedules, component failures, and other events can cause turbines to be temporarily offline [72]. Following literature recommendations, a wind farm availability factor of 95% is assumed, corresponding to a 5% reduction in net energy production [73].

Transmission losses also occur during power delivery via HVDC or HVAC lines, averaging 3.5% per 1000 km for HVDC and 6.7% for HVAC at similar voltage levels [74, 75]. These are modeled using a loss rate λ scaled by distance d_k to the point of connection.

The power output for turbine n in wind farm k, as shown in equation 3.4 integrates these losses.

$$P_{k,n}(v) = P_k(v) \cdot \alpha_{av} \cdot W_e \cdot (1 - d_k \cdot \lambda)\ [\text{MW}], \tag{3.4}$$

where:

- $P_{k,n}(v)$: Power from turbine n in wind farm k at wind speed v [MW].

- α_{av}: Availability factor
- W_e: Wake effect factor (0.85 for 15% wake losses)
- d_k: Distance from wind farm k to conversion station [km]
- λ: Transmission loss rate per km.

Total wind power generation

The total generation across all wind farms considered is then obtained from equation 3.5.

$$P_{\text{wind}}^{\text{gen}}(v) = \sum_{k} \sum_{n=1}^{N_k} P_{k,n}(v) \text{ [MW]}, \tag{3.5}$$

where:

- N_k: Number of turbines in wind farm k.
- $P_{\text{wind}}^{\text{gen}}(v)$: Total generated wind power at wind speed v [MW].

Capacity factor

The capacity factor is a critical performance metric that quantifies the actual energy output of a wind farm relative to its theoretical maximum production [23]. Expressed as a percentage, the capacity factor of a wind farm is calculated, as given in equation 3.6, as the ratio of the total energy generated over a year to the theoretical maximum energy output for the same period [55].

$$CF_{wf} = \frac{\sum_{t=1}^{8760} P_{\text{wind}}^{\text{gen}}(t) \cdot \Delta t}{P_{\text{wind}}^{\text{nom}} \cdot 8760} \cdot 100 \quad [\%] \tag{3.6}$$

where:

- CF_{wf}: Wind farm capacity factor [%]
- $P_{wind}^{gen}(t)$: Wind farm power generation at time t [MW]
- Δt: Time step duration [h]
- P_{wind}^{nom}: Nominal wind farm capacity [MW].

The capacity factor serves as a key indicator for assessing the performance the wind farm model. Offshore wind farms typically achieve annual capacity factors in the range of 40-50%, attributed to the stronger and more consistent wind resources found in marine environments compared to onshore sites [23]. As part of the validation process, the computed capacity factor is used to verify the assumptions made in the power production estimation for the case study, ensuring that the simulated output aligns with established industry benchmarks.

3.3.2 MILP model for energy arbitrage

In this section, the mathematical framework for the energy management system (EMS) configuration is presented, which optimises the operation of the BESS integrated with wind power generation to maximise revenue through energy arbitrage. Energy arbitrage involves storing electricity during periods of low market prices and discharging it to the grid when prices are high [57, 76]. The EMS determines the charging power, discharging power, and manages power flows to achieve this objective.

Model assumptions and scope

The optimization framework is based on several key assumptions that define the system's operational boundaries. A fundamental design parameter is the BESS charging protocol, which restricts the battery to charge only from the offshore wind farm's generation, without drawing energy from the grid. This ensures that the BESS operates using renewable energy and avoiding potentially fossil fuel-based grid electricity.

Also, the battery is assumed to operate under controlled environmental conditions, with cell temperatures maintained at 25 °C, as is standard in many BESS modeling studies for arbitrage applications [55, 56].

In addition, all the energy generated by the wind turbines is either injected into the grid or used to charge the BESS, except during time periods when the DAM electricity price is negative, in which case curtailment is assumed.

Finally, it is assumed unconstrained grid injection, meaning the BESS can always discharge to the grid without facing capacity or congestion limits. This assumption is justified because the BESS typically discharges when DAM prices are high, which aligns with peak system demand [77]. During these periods, grid operators actively seek additional supply, making congestion unlikely.

Objective function

The primary goal of the optimization is to maximize the total system profitability over the optimization horizon T using energy arbitrage. Initially, without considering degradation, the objective focuses solely on revenue maximization as expressed in equation 3.7:

$$\max \sum_{t=1}^{T} (\mathcal{R}_{\text{wind}} + \mathcal{R}_{\text{BESS}}) \quad [€] \tag{3.7}$$

where $\mathcal{R}_{\text{wind}}$ is the revenue from direct wind sales to the grid, calculated following equation 3.8:

$$\mathcal{R}_{\text{wind}} = \sum_{t=1}^{T} \lambda(t) \cdot P_{\text{wind}}^{\text{grid}}(t) \cdot \Delta t \quad [€] \tag{3.8}$$

with $\lambda(t)$ the electricity price at time t in €/MWh, $P_{\text{wind}}^{\text{grid}}(t)$ the wind power, in MW, discharged to the grid at time t, and Δt the time step duration in hours.

Similarly, $\mathcal{R}_{\text{BESS}}$ is the revenue from BESS discharges, and it is calculated following equation 3.9:

$$\mathcal{R}_{\text{BESS}} = \sum_{t=1}^{T} \lambda(t) \cdot P_{\text{BESS}}^{\text{dh}}(t) \cdot \Delta t \quad [€] \tag{3.9}$$

where $P_{\text{BESS}}^{\text{dh}}(t)$ is the power discharged by the BESS in MW.

However, an objective function focused solely on maximizing revenue can lead to excessive cycling by the optimizer, prematurely degrading the battery and ultimately reducing the system's economic value over its operational lifetime. Following common practice in literature [55, 56, 57, 78, 79], the objective function, as shown in equation 3.10, incorporates a degradation cost term $\mathcal{C}_{\text{aging}}$, which penalizes operations that cause significant wear.

$$\max \sum_{t=1}^{T} (\mathcal{R}_{\text{wind}} + \mathcal{R}_{\text{BESS}} - \mathcal{C}_{\text{aging}}) \quad [€] \tag{3.10}$$

This updated formulation explicitly captures the trade-off: higher revenues from aggressive BESS utilization (e.g., frequent charging/discharging during price peaks) are offset by increased degradation costs, which represent the economic impact of capacity loss over time. As such, $\mathcal{C}_{\text{aging}}$ accounts for cycling degradation as a proxy in the objective function, while both cycling and calendar effects dynamically update the available capacity. This approach ensures that optimal solutions balance immediate profitability with sustainable operations, avoiding scenarios where short-term gains erode long-term viability.

Battery degradation model

To ensure the long-term sustainability of operation, the model incorporates battery degradation effects. As discussed in Section 2.3.2, degradation is categorized into cycling degradation from charge-discharge cycles and calendar degradation from time, temperature, and state of charge. Both degradation mechanisms contribute to a gradual decline in the battery's available energy capacity. In the model, this loss of capacity is continuously tracked and used to update the remaining storage capability of the battery energy storage system (BESS) throughout the simulation.

Cycling degradation

The model evaluates cycling degradation through full equivalent cycles (FEC), which represent the energy throughput as equivalent complete charge-discharge cycles. At each time step, when the battery undergoes charging or discharging, the model calculates the instantaneous cycles to track the state of health (SoH) in real time. The equivalent full cycle throughput at each time step is given by equation 3.11 [56].

$$\tau(t) = \frac{P_{\text{BESS}}^{\text{ch}}(t) + P_{\text{BESS}}^{\text{dh}}(t)}{2 \cdot E_{\text{nom}}} \cdot \Delta t \quad [\text{cycles}] \tag{3.11}$$

where $\tau(t)$ is the equivalent full cycle throughput, $P^{\text{ch}}_{\text{BESS}}(t)$ [MW] is the charging power, $P^{\text{dh}}_{\text{BESS}}(t)$ [MW] is the discharging power, E_{nom} [MWh] is the nominal battery capacity, and Δt is the time step duration.

The cumulative equivalent full cycles up to time step t are calculated as:

$$\text{cyc}_{\text{cum}}(t) = \sum_{i=1}^{t} \tau(i) \quad [\text{cycles}] \tag{3.12}$$

Having the equivalent full cycles at each time step, the state of health is modeled and computed accordingly to track the battery's degradation in real-time. The relationship between FEC and SOH is derived from the study by [55], which employs the same battery type (lithium NMC) and similar storage conditions (25 °C temperature). From their experimental results, a maximum cycle life of approximately 6,000 equivalent full cycles is estimated to occur when the battery's EOL reaches the 70% threshold. This degradation analysis forms the basis of the degradation modeling approach adopted in this thesis.

The degradation profile, as shown in Figure 3.3, is characterized by a polynomial relationship with respect to the number of cycles performed. The state of health as a function of cumulative cycles cyc_{cum}, at time, t is expressed as is described by equation 3.13 [55].

$$\begin{aligned} \text{SOH}(t) = 100 &- 5.613^{-32} \cdot \text{cyc}_{\text{cum}}(t)^9 + 3.121^{-27} \cdot \text{cyc}_{\text{cum}}(t)^8 \\ &- 6.353^{-23} \cdot \text{cyc}_{\text{cum}}(t)^7 + 6.630^{-19} \cdot \text{cyc}_{\text{cum}}(t)^6 \\ &- 3.987^{-15} \cdot \text{cyc}_{\text{cum}}(t)^5 + 1.435^{-11} \cdot \text{cyc}_{\text{cum}}(t)^4 \\ &- 3.070^{-8} \cdot \text{cyc}_{\text{cum}}(t)^3 + 3.746^{-5} \cdot \text{cyc}_{\text{cum}}(t)^2 \\ &- 0.0277 \cdot \text{cyc}_{\text{cum}}(t) \quad [\%] \end{aligned} \tag{3.13}$$

The economic impact of cycling degradation is captured in the objective function by introducing an aging cost per equivalent full cycle, as shown in equation 3.14 [56]:

$$\gamma_{\text{deg}} = \frac{E_{\text{nom}} \cdot c^{\text{aging}}}{\text{FEC}^{\text{EOL}}} \quad [€/\text{cycle}] \tag{3.14}$$

where γ_{deg} is the aging cost per cycle, c^{aging} is the degradation cost per unit of lost capacity (adjusted as a percentage of the initial capital expenditure based on desired conservatism in battery usage), and FEC^{EOL} represents the total equivalent full cycles at EOL.

The total cycling degradation cost over the operational period, given by equation 3.15 and 3.16, is computed by aggregating the per-cycle costs as described in [56].

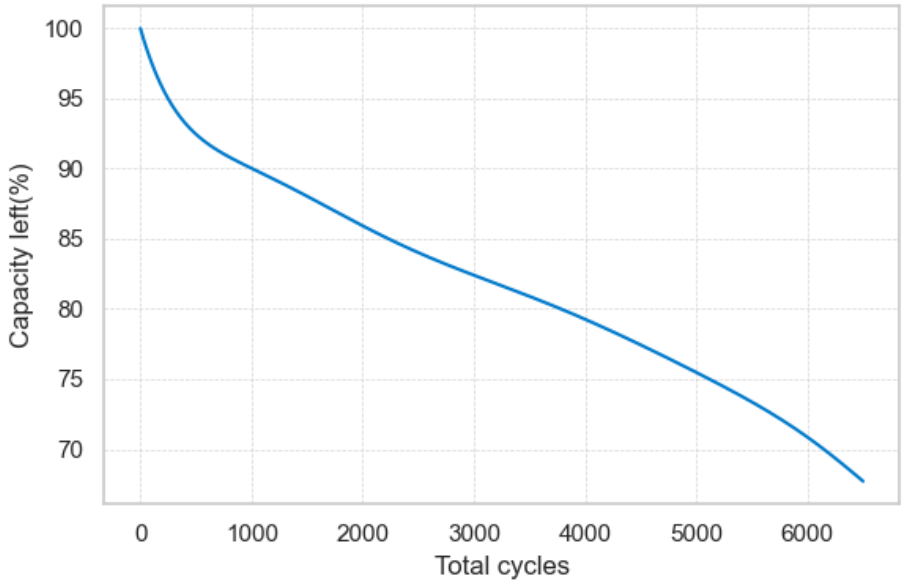

Figure 3.3: Battery degradation profile vs. cycle count

$$\mathcal{C}_{\text{aging}} = \sum_{t=1}^{T} \tau(t) \cdot \gamma_{\text{deg}} \cdot \Delta t \quad [€] \tag{3.15}$$

$$= \sum_{t=1}^{T} \frac{(P^{\text{ch}}_{\text{BESS}}(t) + P^{\text{dh}}_{\text{BESS}}(t)) \cdot \Delta t \cdot c^{\text{aging}}}{2 \cdot \text{FEC}^{\text{EOL}}} \quad [€] \tag{3.16}$$

Calendar degradation

For calendar degradation, the model assumes a simple constant degradation rate to represent the gradual capacity loss over time. Following [80], the constant hourly calendar degradation is expressed by equation 3.17.

$$\text{Cal}_{\text{deg}}(t) = \text{SOC}_{\text{average}} \cdot \frac{1.2 \times 10^{-4}}{24} \quad [\%] \tag{3.17}$$

where $\text{Cal}_{\text{deg}}(t)$ represents the calendar degradation during hour t, and $\text{SOC}_{\text{average}}$ is the average state of charge (SOC) of the battery over its lifetime. In accordance with [80] and [13], the adopted model for this study assumes an average SOC of 50% at 25 °C.

The overall degradation at time t is then obtained, in line with the approach of [10] and [79], as expressed in equation 3.18.

$$\text{Deg}_{\text{total}}(t) = \max\left\{\text{Cyc}_{\text{deg}}(t), \text{Cal}_{\text{deg}}(t)\right\} \quad [\%] \tag{3.18}$$

where $\text{Deg}_{\text{total}}(t)$ represents the total degradation, $\text{Cyc}_{\text{deg}}(t)$ is the cycling degradation as a function of equivalent full cycles, and $\text{Cal}_{\text{deg}}(t)$ is the calendar degradation, all at time t.

System constraints

The model includes constraints to ensure feasible and realistic operations of the integrated wind-BESS system.

Power balance: The power balance constraint, expressed by equation 3.19, allocates wind generation between grid sales, BESS charging, and losses, at each time step.

$$P_{\text{wind}}^{\text{gen}}(t) = P_{\text{wind}}^{\text{grid}}(t) + P_{\text{BESS}}^{\text{ch}}(t) + P_{\text{wind}}^{\text{loss}}(t) \quad [\text{MW}] \tag{3.19}$$

where $P_{\text{wind}}^{\text{gen}}$ is the net wind power generated from the offshore wind farm, $P_{\text{BESS}}^{\text{ch}}$ is the BESS charging power, and $P_{\text{wind}}^{\text{loss}}(t)$ accounts for wind power losses due to curtailment.

Power Rating Boundaries: As shown in equations 3.20 and 3.21, charging and discharging are bounded by the rated power.

$$0 \leq P_{\text{BESS}}^{\text{ch}}(t) \leq P_{\text{rated}} \cdot \delta_{\text{ch}}(t) \quad [\text{MW}] \tag{3.20}$$

$$0 \leq P_{\text{BESS}}^{\text{dh}}(t) \leq P_{\text{rated}} \cdot \delta_{\text{dh}}(t) \quad [\text{MW}] \tag{3.21}$$

where P_{rated} is the rated power, and δ_{ch} and δ_{dh} are binary variables that indicate the charging and discharging modes, respectively.

Operational mode constraint: To limit degradation, simultaneous charging and discharging is not allowed. This is implemented following equation 3.22

$$\delta_{\text{ch}}(t) + \delta_{\text{dh}}(t) \leq 1 \tag{3.22}$$

State of charge (SOC) range: Equation 3.23 is used to bound the SOC to preserve battery health:

$$\text{SOC}_{\text{min}} \leq \text{SOC}(t) \leq \text{SOC}_{\text{max}} \quad [\text{MWh}] \tag{3.23}$$

where SOC_{min} and SOC_{max} are the minimum and maximum SOC levels, defined in this thesis as 20% and 90% of the available capacity respectively. This is expressed by the equations 3.24 and 3.25.

$$\text{SOC}_{\text{min}} = 0.20 \cdot E_{\text{available}}(t) \quad [\text{MWh}] \tag{3.24}$$

$$\text{SOC}_{\text{max}} = 0.90 \cdot E_{\text{available}}(t) \quad [\text{MWh}] \tag{3.25}$$

and $E_{\text{available}}(t)$ is the available capacity at time t.

Energy storage evolution

The state of charge (SOC) evolution tracks stored energy, accounting for efficiencies and losses. For the initial time step, the SOC is expressed following equation 3.26.

$$\text{SOC}(1) = \text{SOC}_{\text{initial}} + \left[P_{\text{BESS}}^{\text{ch}}(1) \cdot \eta_{\text{ch}} - \frac{P_{\text{BESS}}^{\text{dh}}(1)}{\eta_{\text{dh}}} \right] \cdot \Delta t \quad [\text{MWh}] \tag{3.26}$$

where SOC(1) is the state of charge at time step 1, $\text{SOC}_{\text{initial}}$ is the initial state of charge, η_{ch} is the charging efficiency, and η_{dh} is the discharging efficiency.
For subsequent time steps, the SOC is expressed following equation 3.27.

$$\text{SOC}(t) = \text{SOC}(t-1) + \left[P^{\text{ch}}_{\text{BESS}}(t) \cdot \eta_{\text{ch}} - \frac{P^{\text{dh}}_{\text{BESS}}(t)}{\eta_{\text{dh}}} \right] \cdot \Delta t \quad [\text{MWh}] \tag{3.27}$$

where $\text{SOC}(t)$ is the state of charge at time t.

Implementation

The proposed mathematical framework was implemented in Python using the *Pyomo* framework for MILP formulation and solved using the GLPK solver discussed in Section 2.5.3. The implementation follows the structured workflow depicted in the methodology flowchart, Figure 3.4.

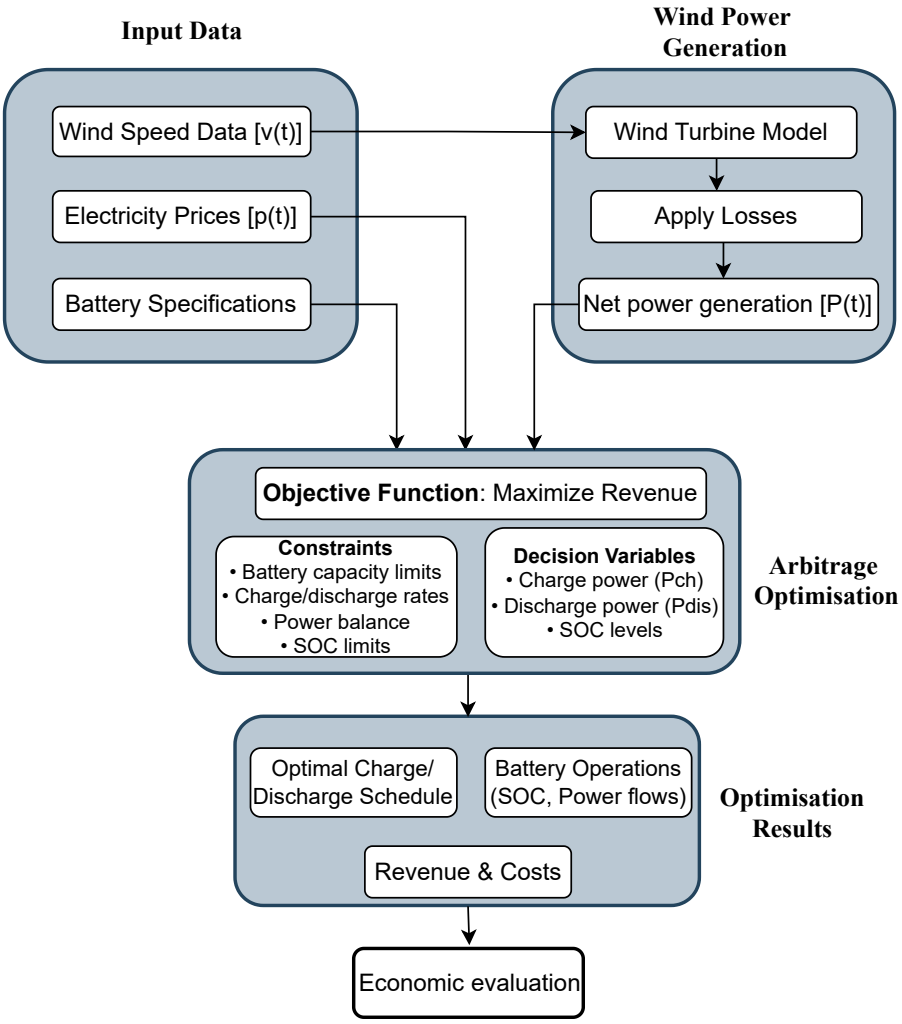

Figure 3.4: BESS methodology flowchart

Model setup: BESS parameters were first defined, including nominal capacity, power rating, efficiencies, and degradation coefficients. The model imports wind

power forecasts and electricity price data over a specified time period with hourly resolution. The time step duration is set to $\Delta t = 1$ hour, aligning with the resolution of the input data.

Optimization loop: The core optimization process is modeled as a MILP that uses an MPC approach to maximize revenue while adhering to the operational constraints detailed in Section 3.3.2. The algorithm employs a rolling time horizon of 24 hours with hourly time steps. At each time step, the optimization determines optimal charging/discharging decisions while anticipating future wind generation and price conditions. The battery's state of charge and capacity are updated based on the optimization results and degradation calculations according to the formulations in Section 3.3.2. The total profit was computed after completing the optimization across the entire planning horizon.

Outputs: The process iterated across the optimization horizon, accumulating revenues and costs to compute total profit. Outputs included charge and discharge profiles, SOC evolution, degradation progression, and economic metrics.

3.4 Economic evaluation framework

3.4.1 BESS cost analysis

The economic feasibility of deploying a BESS requires a clear overview of the associated investment costs. The primary cost factors for BESS deployment are discussed in the following sections.

Capital expenditures (CAPEX)

The CAPEX cover the initial investment for establishing a BESS, including equipment and installation costs. These costs are expressed in terms of power capacity (€/kW) or energy capacity (€/kWh), depending on the analysis [10, 51]. The total system cost comprises the lithium battery pack and its supporting infrastructure, known as the balance of system (BOS) [81]. The BOS includes power electronics, such as inverters, transformers, cooling systems, and wiring [82]. The lithium battery pack typically accounts for about 50% of the total BESS capital expenditure [83]. For utility-scale lithium-ion BESS applications, current CAPEX is estimated at 200–400 $/kWh [84][1]. Future cost reductions are anticipated due the combined effects of R&D innovations and economies of scale [81, 86].

Operational expenditures (OPEX)

OPEX represents the costs associated with the normal operation of a BESS, encompassing maintenance and operational expenses [82, 87]. OPEX is typically expressed as an annual cost per unit of installed power capacity (€/kW/year) [51]. These costs

[1] Approximately 184–367 €/kWh based on April 2025 exchange rate [85]

are typically divided into fixed operation and maintenance (FOM) costs, which depend on the installed capacity, and variable operation and maintenance (VOM) costs, which vary with the amount of electricity stored [29, 81]. For the sake of simplicity, this thesis only considers FOM costs, while neglecting costs from VOM.

Replacement costs

As discussed in section 2.3.2, battery usage leads to degradation, reducing energy storage capacity over time. When the battery reaches its EOL threshold, replacement becomes necessary to maintain system efficiency and profitability [10]. This constitutes the most significant cost after initial installation costs [10]. In this thesis, replacement costs are assumed to be 50% of the initial CAPEX, reflecting anticipated advancements in battery technology and manufacturing efficiency by 2030. This estimate accounts for the renewal of storage modules and associated storage-related BOS components, while assuming that existing cabling and control systems remain operational [83]. This assumption is consistent with recent projections indicating that lithium-ion battery costs could decline substantially within the next decade, by up to 65% by 2030 [86].

Cost summary

Table 3.1 summarizes the main cost assumptions used in this thesis for the BESS project.

Table 3.1: Summary of BESS cost parameters

Cost Component	Value	Unit	Source
$CAPEX^{BESS}$	200	€/kWh	[88]
$CAPEX^{BOS}$	250	€/kW	[88]
OPEX	1.5	% of CAPEX/year	[89]
Replacement	50	% of initial CAPEX	[86, 90]

3.4.2 Financial metrics

The financial performance of BESS will be evaluated using established economic metrics. These indicators assess profitability, cost recovery, and the overall attractiveness of investments. The methods applied in this study are discussed in the following sections:

Net present value (NPV)

The NPV is a key financial metric used to assess the profitability of BESS projects by evaluating the present value of all cash inflows and outflows over the project's lifetime [38, 91, 92]. As previously seen, the costs incurred in the BESS include the CAPEX, replacement, O&M, and end-of-life costs. The NPV is calculated by subtracting the sum of these discounted costs from the sum of discounted revenues, as expressed in equation 3.28 [38].

$$NPV = \sum_{n}^{N} \frac{revenue(n) - cost(n)}{(1+r)^n} \quad [€] \tag{3.28}$$

$$= \sum_{n=0}^{N} \frac{revenue(n)}{(1+r)^n} - \sum_{n}^{N} \frac{CAPEX + replacement + O\&M}{(1+r)^n} \quad [€] \tag{3.29}$$

where,

- r: The discount rate.
- N: The project lifetime.

A positive NPV indicates that the project's expected earnings exceed its costs, making it economically viable, while a negative NPV suggests a financial loss [91, 93]. The choice of the discount rate is a decisive factor in NPV analysis, as it can substantially influence the result. Its value is context dependent, shaped by the nature of the investment and the return expectations of its stakeholders [90]. A common reference point is the weighted average cost of capital (WACC) [38, 94], which is entity-specific and represents the average return required by debt and equity holders, weighted by their proportion in the capital structure [29, 92].

Internal rate of return (IRR)

The IRR is the discount rate at which the NPV of a project equals zero, indicating the project's potential profitability [10, 91]. It's a useful tool for comparing alternative investment opportunities [92]. It is calculated by setting the NPV formula to zero and solving for the discount rate, as shown in equation 3.30 [38].

$$NPV = 0 = \sum_{n=1}^{N} \frac{revenue(n) - cost(n)}{(1+IRR)^n} \quad [€] \tag{3.30}$$

The higher the IRR, the more attractive a project is to investors [92]. In general, a project is considered financially viable if its IRR exceeds the prevailing discount rate [91, 93, 95]. In this thesis, a discount rate of 7% is used, consistent with regulated benchmarks in the electricity generation sector [96]. Projects with an IRR above this level are regarded as financially attractive, while those below 7% are not considered financially viable.

Payback period

The payback period represents the time required for a project to recover its initial investment through cumulative cash flows [38, 94]. For projects with constant cash flows, it is calculated using equation 3.31 [38].

$$Payback\ period = \frac{Initial\ investment}{Annual\ cash\ flow} \quad [\text{years}] \tag{3.31}$$

However, energy storage projects typically have variable cash flows, necessitating models to track cash inflows and outflows over time [38]. The discounted payback

period (DPP) discounts future cash flows before summing them until the initial investment is recovered [38, 93].

3.4.3 Sensitivity analysis

The economic evaluation of the BESS project includes a sensitivity analysis to ensure its reliability. This analysis systematically varies key input parameters such as CAPEX, OPEX, discount rate, market prices, and round-trip efficiency (RTE) of the BESS. The goal is to assess the impact of changes in these factors on the NPV, IRR, and PBT outcomes. This analysis helps to identify the most influential variables affecting project viability, thereby supporting better decision-making to improve design and reduce uncertainty.

3.5 Case study description

3.5.1 Overview of the BorWin2 project

The BorWin2 project located in the North Sea will serve as the case study to this thesis. This project, developed by TenneT, is a HVDC system with a transmission capacity of 800 MW, specifically designed to integrate offshore wind energy into the German electricity grid. Operational since January 2015, BorWin2 connects three distinct offshore wind farm clusters: *Deutsche Bucht*, *Albatros*, and *Veja Mate*, all located in the North Sea, with a total capacity of approximately 774 MW. Electricity is transmitted over a 200 km route, consisting of a 125 km submarine cable from the offshore converter platform to the landing point at Hilgenriedersiel, followed by a 75 km underground cable to the onshore converter station at Diele (see Figure 3.5). The wind farms' AC output is collected at their transformer stations, transmitted via 155 kV AC cables to the BorWin beta platform, converted to DC, and then delivered to the mainland for conversion back to AC [21]. A summary of the key characteristics of each offshore wind farm cluster, including turbine types, number of turbines, rotor diameter, and hub height, is presented in Table 3.2 [66, 67, 97, 98, 99, 100, 101, 102].

Table 3.2: Technical Specifications of Selected offshore wind farms

Parameter	**Deutsche Bucht**	**Albatros**	**Veja Mate**
Turbine type	MHI Vestas V164-8.4MW	Siemens SWT-7.0-154	Siemens SWT-6.0-154
Turbine power [MW]	8.4	7	6
Number of turbines	31	16	67
Total power [MW]	260.4	112	402
Distance to platform [km]	41	25	12
Turbine cut-in speed [m/s]	4	3	4
Turbine cut-out speed [m/s]	25	25	25
Turbine rated speed [m/s]	13	13	13
Rotor diameter [m]	164	154	154
Hub height above sea [m]	100	105	80

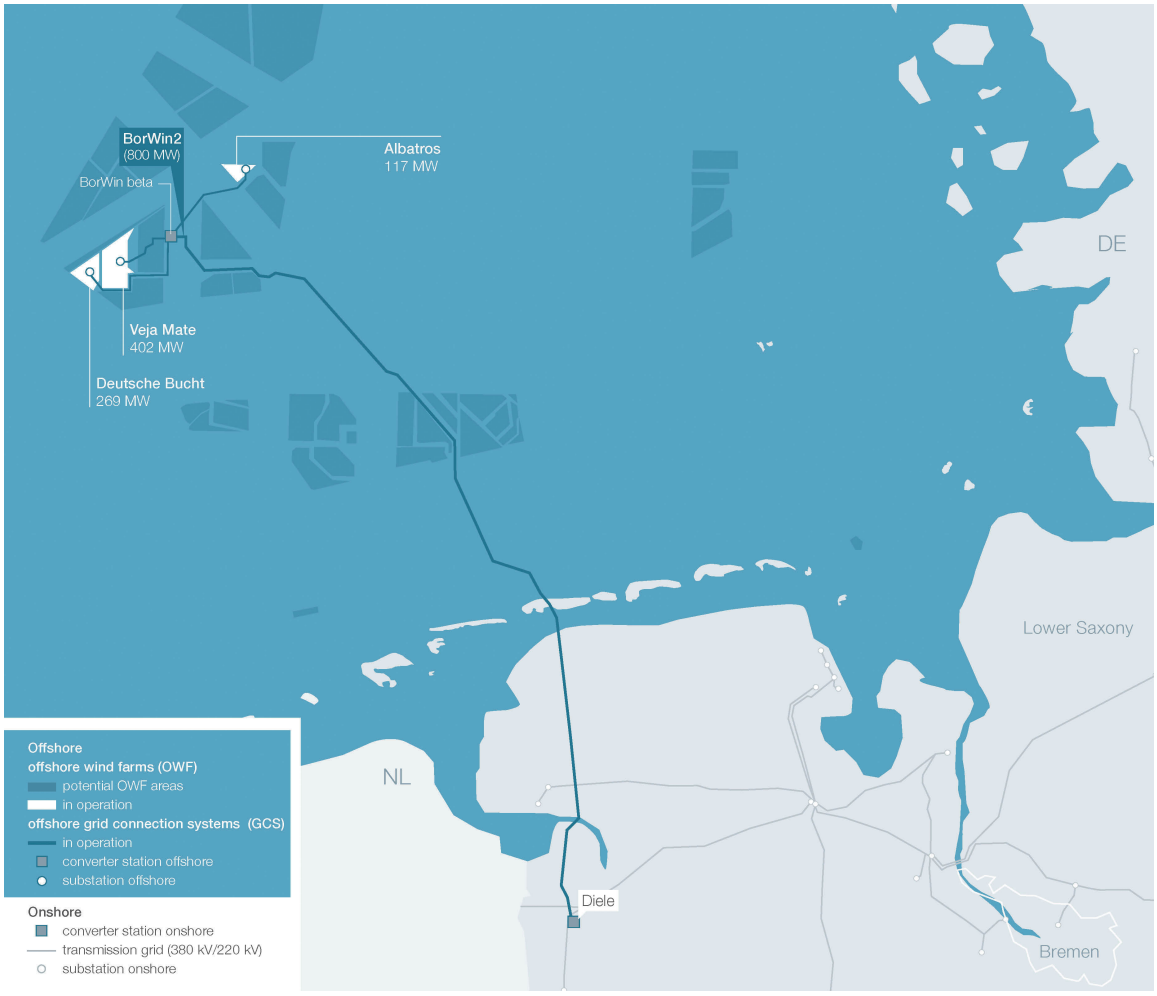

Figure 3.5: Schematic of the BorWin2 platform and connected offshore wind clusters [21]

In order to estimate the energy production of the offshore wind farm cluster, wind speed data were calculated for a representative location (54.38°N, 6.02°E), determined by averaging the coordinates of *Deutsche Bucht* (54.31°N, 5.80°E) [97], *Albatros* (54.50°N, 6.40°E) [98], and *Veja Mate* (54.32°N, 5.87°E) [99]. These wind speed time series were combined with turbine-specific power curves to estimate the energy output of the cluster, as detailed in Section 3.3.1.

Power curves for the *Veja Mate* turbines (Siemens SWT 6.0-154) were directly sourced from [66]. For the *Albatros* turbines (Siemens SWT-7.0-154), which lacked publicly available data, the power curves were scaled from the *Veja Mate* turbines' curves due to the similarities in design. Similarly, the *Deutsche Bucht* turbines' power curves (MHI Vestas V164-8.4MW) were derived by scaling from the MHI Vestas V164-8MW turbine power curves [67] (see Appendix A).

3.5.2 BESS specifications and assumptions

The integration of a battery energy storage system (BESS) into the model under consideration is critical, as it directly influences the economic evaluation framework of the case study. Hence, the following sections specify the BESS configuration and assumptions adopted in this thesis to ensure accurate modeling of its performance and economic impact.

Power rating and sizing

A thorough investigation of the optimal sizing of the BESS is beyond the scope of this study. Instead, the power rating is determined based on insights from [103], which observes that the optimal BESS capacity is approximately 16% of the daily electricity generation at the full capacity of the offshore wind farm. For the wind farm under study, with a rated capacity of approximately 774 MW, this translates to a BESS power rating of about 125 MW.

Energy capacity and storage durations

To determine the optimal storage duration for arbitrage operations, the BESS is modeled with four distinct scenarios, featuring storage durations of 1, 2, 4, and 5 hours. With a fixed power rating of 125 MW, these scenarios correspond to energy capacities of 125 MWh, 250 MWh, 500 MWh, and 625 MWh, respectively. These configurations allow the model to identify the most economically viable storage duration.

Battery technology and performance characteristics

In this thesis, the BESS is assumed to utilize Lithium Nickel Manganese Cobalt Oxide (NMC) battery cells and operate under a controlled ambient temperature of 25 °C, in alignment with [55]. These parameters are selected to align with the battery degradation profile from [55], which is used in the BESS model, ensuring consistent simulation of its performance. A round-trip efficiency of 90% is also adopted, consistent with representative figures found in relevant literature [10, 54]

Project lifetime and battery replacement

For this case study, the operational lifetime of the battery energy storage system (BESS) is assumed to be 18 years. This estimate is based on the BESS's performance and degradation profile. However, this lifetime may vary slightly depending on cycle degradation, which is influenced by the frequency and intensity of charge-discharge cycles associated with arbitrage activities. Consistent with [55], the battery's End-of-Life (EOL) is defined when its capacity degrades to 70% of its initial nominal value. The model also assumes a one-time battery replacement during the project lifetime.

Chapter 4

Results

This chapter presents the results obtained from the simulations and economic evaluations conducted in this study. The results are structured to first provide an overview of the wind power generation, followed by the BESS's operational behavior, an annual performance evaluation across different years, a comparison of storage durations for the selected representative year, a comparison between onshore and offshore BESS configurations, and finally the sensitivity analysis.

4.1 Wind power generation

The wind power generation model was validated using capacity factors for the three offshore wind farms: *Deutsche Bucht, Veja Mate*, and *Albatros*. Table 4.1 summarizes the annual capacity factors for the years 2021 to 2024. These values align with literature expectations for offshore wind farms, typically ranging from 40-50% [23]. It should be noted that real production data for these specific wind farms is not publicly available, so validation relies on literature benchmarking.

Table 4.1: Annual capacity factors for the wind farms

Year	**Deutsche Bucht (%)**	**Veja Mate (%)**	**Albatros (%)**
2021	44.14	41.72	40.60
2022	47.86	45.35	44.22
2023	46.42	43.87	42.82
2024	48.35	45.70	44.57

The power generation profiles exhibit seasonal variations, with higher outputs during winter months due to stronger winds. For instance, Figure 4.1 illustrates the hourly power output for December 2023, a representative winter month, where the case study wind farm cluster achieves an average power production of approximately 448 MW. In contrast, Figure 4.2 shows the hourly power output for August 2023, a representative summer month, with lower wind speeds resulting in an average production of around 208 MW.

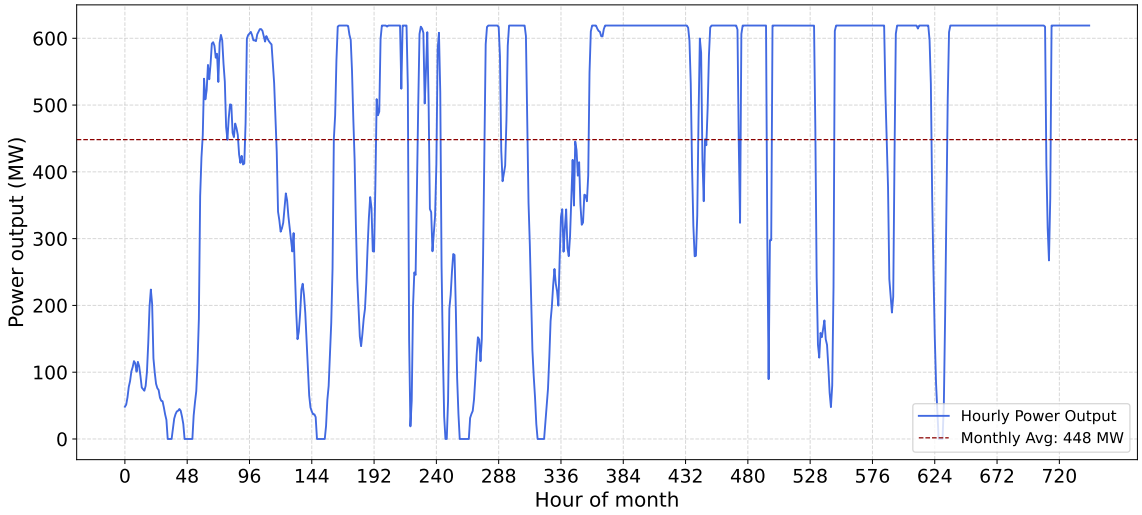

Figure 4.1: Wind power generation profile for a representative winter month

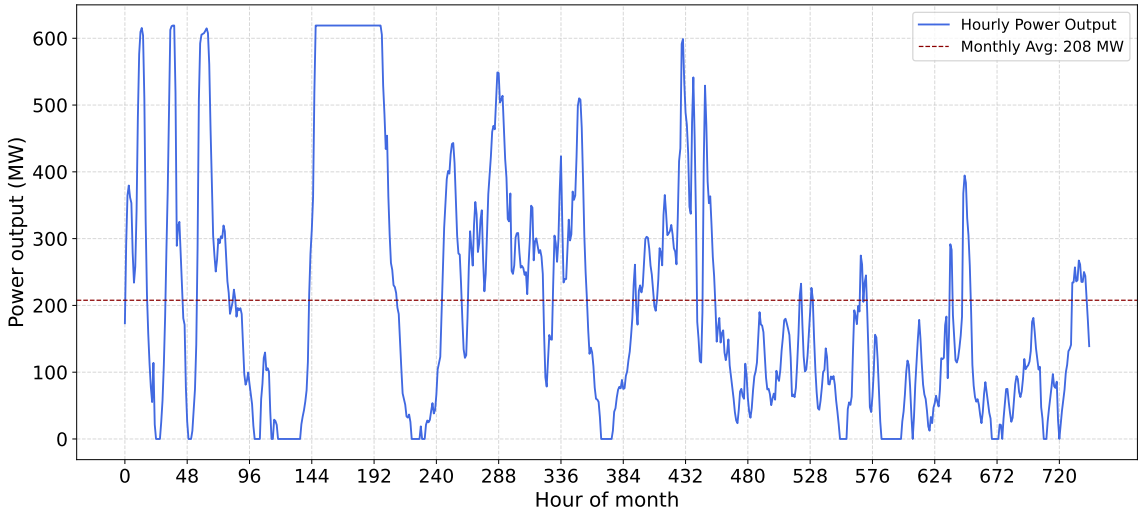

Figure 4.2: Wind power generation profile for a representative summer month

4.2 Energy arbitrage operation overview

The analyzed battery energy storage system (BESS) has a fixed power rating of 125 MW, with energy capacities varying based on storage duration, such as 125 MWh for a 1-hour duration, 250 MWh for a 2-hour duration, and so forth. For illustrating the operational behavior, a 4-hour storage duration, corresponding to an energy capacity of 500 MWh, is initially considered. The energy arbitrage strategy, implemented via mixed-integer linear programming and model predictive control, optimizes BESS charging and discharging based on wind power forecasts, electricity prices, and current state of charge (SOC).

Figure 4.3 illustrates a representative example of BESS operation over a 72-hour period from December 3 to 5, 2023, depicting SOC evolution alongside DAM price

levels, charging/discharging power patterns, and a comparison between available wind power and power delivered to the grid. The optimization results demonstrate a clear correlation between price signals and storage operation. Charging (shown in green) primarily occurs during below-average price intervals, while discharging (shown in red) occurs mostly during price peaks. These cycling patterns effectively capture arbitrage opportunities while adhering to operational constraints.

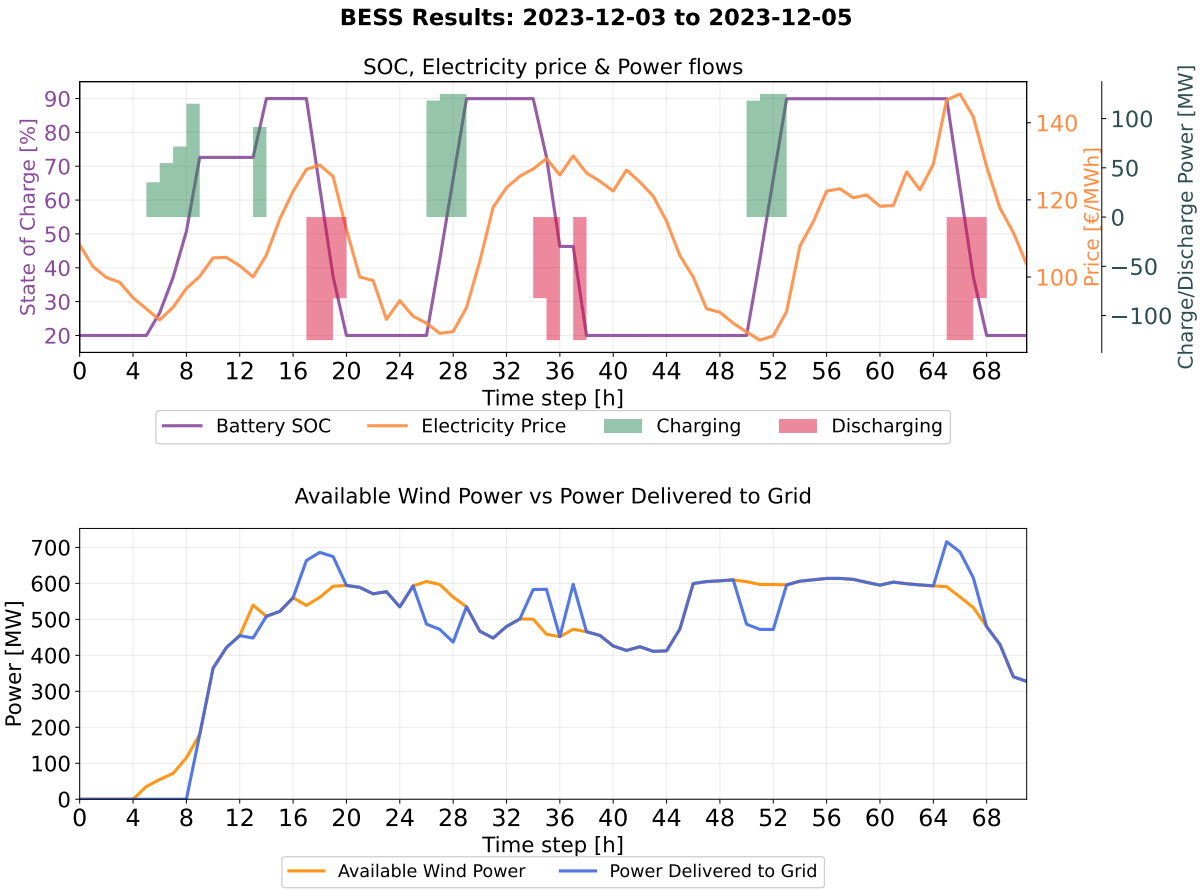

Figure 4.3: Optimal 4-hour BESS operation for energy arbitrage with SOC, electricity price, charging/discharging power, available wind power, and power delivered to the grid (December 3–5, 2023)

The arbitrage operation directly influences the power delivered to the grid relative to the available wind power. When the BESS charges, the total power delivered to the grid (blue line) is reduced compared to available wind power (orange line). Conversely, during discharging periods, the BESS supplements the wind power delivery, resulting in power delivered to the grid exceeding the available wind power, as observed during high-price periods.

4.3 Annual economic performance

The economic performance of the BESS is evaluated using historical data from 2021 to 2024. The discount rate assumed in the simulations is 7%, meaning that an internal rate of return (IRR) below this threshold is non-profitable. Table 4.2 summarizes

the key financial metrics for a 4-hour storage duration (125 MW / 500 MWh) across the years 2021 to 2024.

Table 4.2: Annual performance for a 4-hour storage duration

Year	IRR (%)	NPV (M€)	PBT (years)
2021	5.14	-22.33	21.7
2022	34.29	263.18	5.3
2023	8.07	9.23	16.8
2024	6.24	-6.36	18.9

A quick observation of the results shows that the year 2022 stands out with an exceptionally high IRR of 34.29%, primarily driven by very high price volatility in the energy markets, which was a direct consequence of the gas shortage following the Russian invasion of Ukraine [76]. This effect is evident in the annual average DAM electricity prices, which were around 100 €/MWh in 2021, surged to about 235 €/MWh in 2022, and then returned to roughly 95 €/MWh in 2023 and 79 €/MWh in 2024. Hence, 2022 is not representative of typical market conditions and is excluded from further analysis to avoid over-optimistic conclusions.

For the other years, the project is not strictly profitable with the 4-hour BESS configuration in 2021 and 2024, but 2023 yields an IRR of 8.07%, above the 7% viability threshold. Hence, the year 2023 is selected as the representative base year for a more detailed analysis.

4.4 Impact of BESS duration on profitability

Having established 2023 as the representative year, simulations were performed to determine the optimal BESS storage duration with a fixed power rating of 125 MW. As discussed in Section 2.3.1, storage durations are inversely related to the C-rate: shorter durations correspond to higher C-rates, enabling rapid energy dispatch, while longer durations align with lower C-rates, supporting sustained energy delivery. The economic results, including the corresponding energy capacities and C-rates, are detailed in Table 4.3.

Table 4.3: Financial performance for different storage durations in 2023

Duration (hour)	Energy capacity (MWh)	C-rate	IRR (%)	NPV (M€)	PBT (years)
1	125	1C	−7.57	−35.67	38.3
2	250	0.5C	3.28	−16.97	20.2
4	500	0.25C	8.07	9.23	16.8
5	625	0.2C	8.10	11.29	16.8

Simulation results from the case study show that longer storage durations (corresponding to lower C-rates) improve financial returns, while shorter durations (associated with higher C-rates) produce negative NPVs, indicating economic unviability. The 5-hour duration (625 MWh) exhibits the highest profitability, with an IRR of 8.10% and an NPV of 11.29 M€, making it the selected reference case for further analysis. Figure 4.4 illustrates the trends in IRR, NPV and PBT across different storage durations, highlighting improved economic performance as storage duration increases.

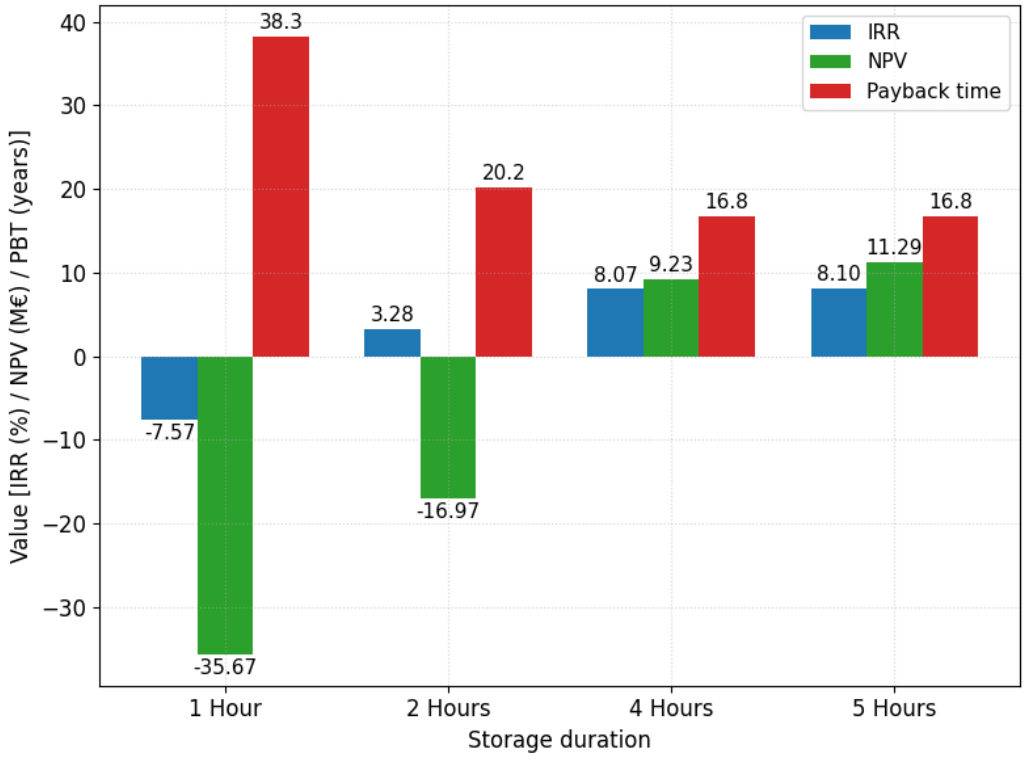

Figure 4.4: Comparison of internal rate of return (IRR), net present value (NPV) and payback time (PBT) across storage durations for 2023

4.4.1 Offshore vs. onshore BESS considerations

The physical location of a BESS significantly influences its economic viability. Although detailed cost data for offshore BESS installations is limited, existing literature suggests that installation and maintenance expenses may be up to 50% higher than for comparable onshore systems [104]. This assumption was applied to the reference case (5-hour storage duration, 2023) in order to compare onshore and offshore scenarios, as summarized in Table 4.4.

Table 4.4: Economic comparison of onshore vs. offshore BESS placement.

Performance metric	**Onshore BESS**	**Offshore BESS**
IRR (%)	8.10	−0.30
NPV (M€)	11.29	−98.48
PBT (years)	16.8	31

The results indicate that with current cost assumptions, an offshore BESS is not economically viable. The 50% increase in CAPEX drastically reduces the IRR to −0.30% and results in a significant negative NPV. Therefore, an onshore location is the only feasible option under the studied conditions.

4.5 Reference case analysis

Based on the preceding analysis, the reference case for this study is an onshore, 125 MW/625 MWh BESS operating under 2023 market conditions. This section presents both the cost structure and operational performance of this reference configuration.

4.5.1 Cost breakdown

The key cost components for this reference project are detailed in Table 4.5. The total initial investment amounts to approximately 156.25 M€, with additional operational and replacement costs distributed over the project lifetime.

Table 4.5: Cost breakdown for the reference case project.

Component	**Cost (M€)**	**Notes**
BESS CAPEX	125	Based on 625 MWh at 200 €/kWh
BOS CAPEX	31.25	Based on 125 MW at 250 €/kW
Total Initial CAPEX	**156.25**	
Annual OPEX	2.34	1.5% of total CAPEX per year
Replacement Cost	78.125	50% of initial CAPEX, once during lifetime

4.5.2 Performance metrics

The performance of the BESS over its lifetime is evaluated based on average operational metrics, including revenue generation, cycling frequency, and degradation rate. These metrics are summarized in Table 4.6.

Table 4.6: Average performance metrics for the reference case

Metric	**Value**	**Notes**
Annual BESS Revenue (M€)	22.70	Average over project lifetime
Annual Cycle Throughput	281	Equivalent to approx. 0.77 cycles per day
Annual Degradation Rate (%)	3.18	Capacity loss per year

Simulation results demonstrate that the BESS reaches its end of life (EOL) after 18 years of operation, with a battery replacement performed after 9 years.

4.6 Sensitivity analysis

This section presents a sensitivity analysis on the reference case to evaluate the impact of key parameters on the internal rate of return (IRR), the net present value (NPV),

and the payback time (PBT). Variations of ±20% are applied to capital expenditure (CAPEX), operational expenditure (OPEX), discount rate, and day-ahead market (DAM) prices. The round-trip efficiency (RTE) is varied from 70% to 100%, and the impact of battery degradation is assessed.

4.6.1 Impact of degradation consideration

To evaluate the impact of battery degradation, a comparative simulation was performed without considering degradation effects and assessed against the case with degradation considerations. The results indicate that battery degradation substantially influences economic performance. As shown in Table 4.7, the net present value (NPV) decreases significantly: from 32.31 M€ in the case without degradation modeling to 11.29 M€ when degradation is taken into account. This difference is further illustrated in Figure 4.5.

Table 4.7: Impact of degradation consideration

Scenario	**IRR (%)**	**NPV (M€)**	**PBT (years)**
With Degradation	8.10	11.29	16.8
Without Degradation	9.97	32.31	15.0

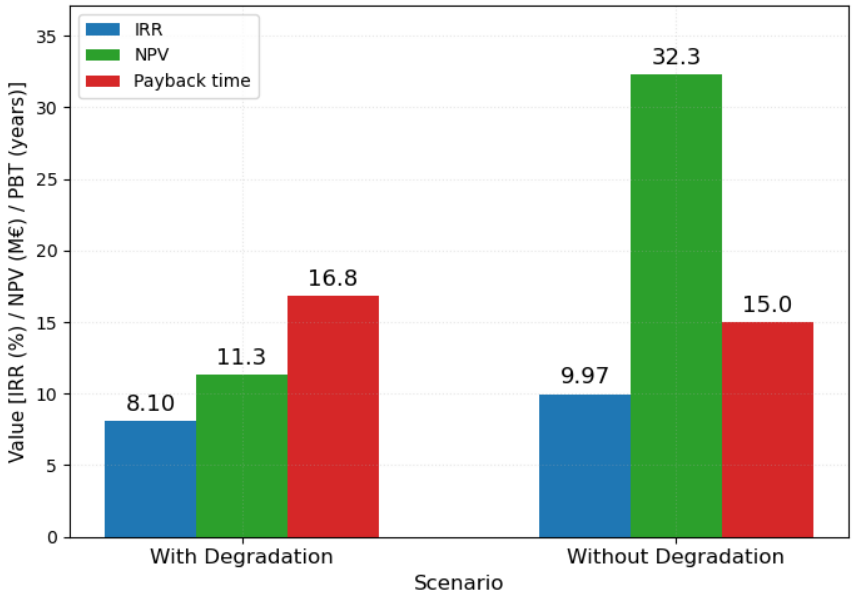

Figure 4.5: Impact of degradation on financial metrics

4.6.2 Sensitivity analysis results

The effects of ±20% parameter variations on IRR, NPV, and PBT are summarized in Table 4.8.

Table 4.8: Sensitivity analysis results for the reference case

Parameter	Variation (%)	IRR (%)	NPV (M€)	PBT (years)
Base case	—	8.10	11.29	16.8
CAPEX	+20	4.20	−32.62	21.8
	−20	13.32	55.20	12.5
OPEX	+20	7.64	6.57	17.3
	−20	8.55	16.00	16.3
Discount rate	+20	8.10	−2.85	18.3
	−20	8.10	27.86	15.3
DAM price	+20	12.92	64.30	12.8
	−20	2.58	−41.90	24.6

4.6.3 Impact on internal rate of return (IRR)

As shown in Figure 4.6, the sensitivity analysis for the internal rate of return (IRR) indicates that it is most sensitive to variations in day-ahead market (DAM) prices, with values ranging from 2.6% to 12.9%, representing a deviation of approximately 5 percentage points in either direction from the base IRR. Capital expenditure (CAPEX) also has a comparable influence, yielding IRR values from 4.20% to 13.32%, or a change of roughly 4 percentage points below and 5 percentage points above the base IRR. In contrast, operational expenditure (OPEX) has a minimal effect, with IRR varying only between 7.64% and 8.55%, reflecting a modest shift of approximately 0.5 percentage points in either direction.

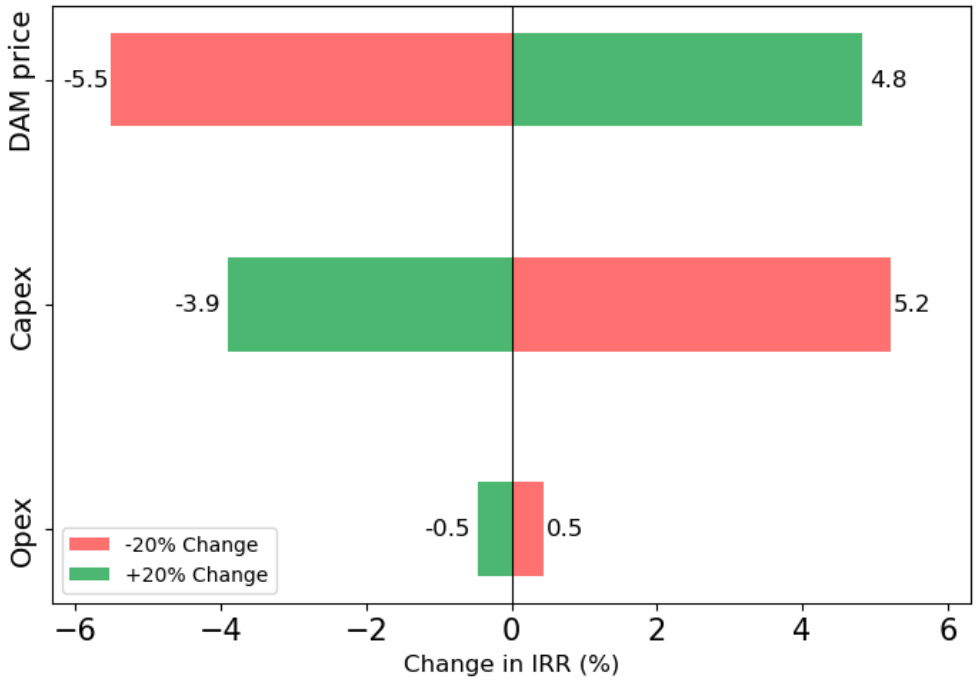

Figure 4.6: Sensitivity analysis for internal rate of return (IRR)

4.6.4 Impact on net present value (NPV)

As illustrated in Figure 4.7, the results indicate that the net present value (NPV) exhibits the greatest sensitivity to variations in day-ahead market (DAM) prices, with NPV ranging from −41.9 M€ to 64.3 M€, equivalent to a deviation of approximately 53 M€ in either direction from the base NPV of 11.29 M€. The CAPEX follows closely in influence, producing NPV values from −32.6 M€ to 55.2 M€, or a change of about 44 M€ in both directions. Sensitivity to the discount rate is comparatively lower, yielding NPV values as low as −2.85 M€ or as high as 27.9 M€. The OPEX, by contrast, exerts a negligible impact, with NPV confined to a narrow band between 6.6 M€ and 16 M€, reflecting a modest variation of roughly 5 M€ in either direction.

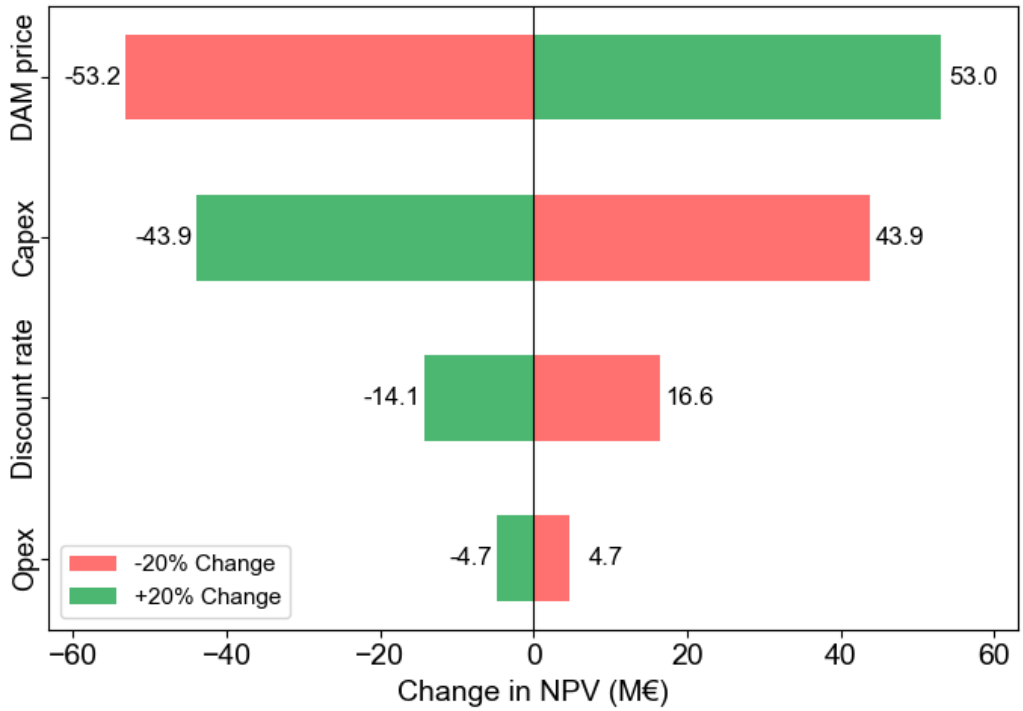

Figure 4.7: Sensitivity analysis for net present value (NPV)

4.6.5 Impact on payback time (PBT)

Regarding the payback time (PBT), as illustrated in Figure 4.8, the results demonstrate the greatest sensitivity to variations in DAM prices, with PBT ranging from 12.8 years to 24.6 years. The CAPEX exhibits comparable sensitivity, yielding PBT values from 12.5 years to 21.8 years, where the higher value likewise surpasses the project lifetime and indicates non-recovery of investment. The discount rate and OPEX exert more limited influences, producing PBT ranges of 15.3 to 18.3 years and 16.3 to 17.3 years, respectively, both of which remain closer to the project duration.

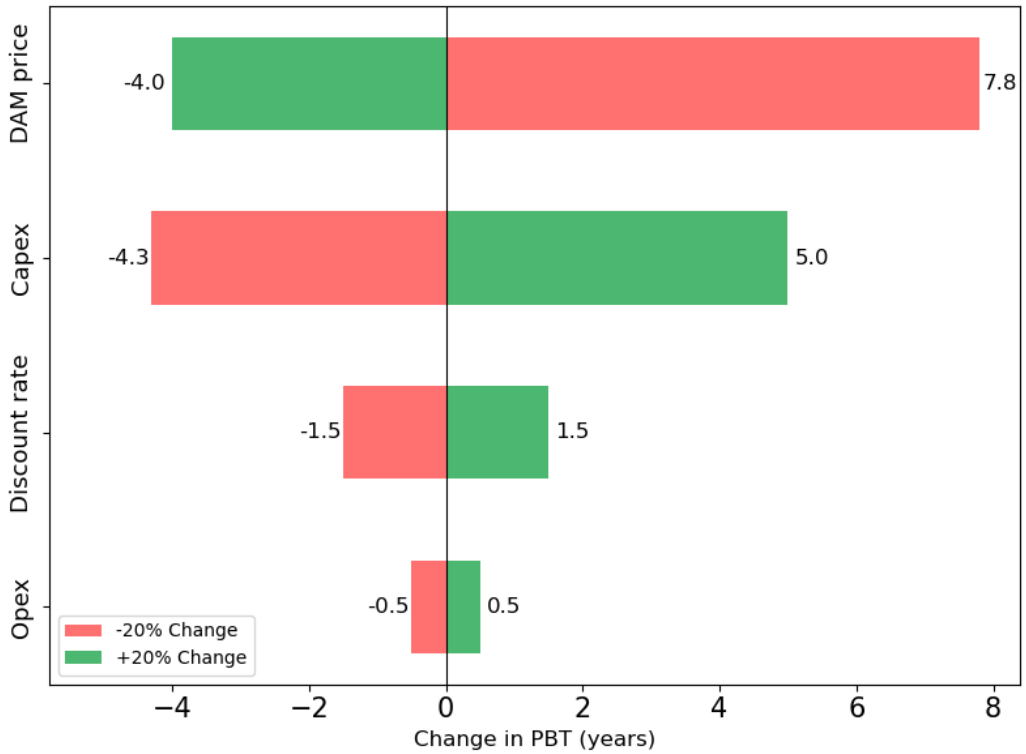

Figure 4.8: Sensitivity analysis for payback time (PBT)

4.6.6 Impact of round-trip efficiency (RTE)

Figure 4.9 shows how variations in RTE from 70% to 100% affect the key financial metrics of the BESS project. As already mentioned, the base case was set at a round-trip efficiency of 90%. At the lower end, with a 70% RTE, the project exhibits a negative NPV of approximately −95.5 M€ and a negative IRR of −3.7%, alongside a lengthy payback time exceeding 50 years. As RTE improves, these metrics steadily move toward positive values and shorter payback periods. Compared to the base case, increasing RTE to 95% and 100% significantly enhances performance, with NPVs reaching 31.8 M€ and 50.8 M€, IRRs rising to 10.0% and 11.7%, and payback times decreasing to 15 and 13.6 years, respectively.

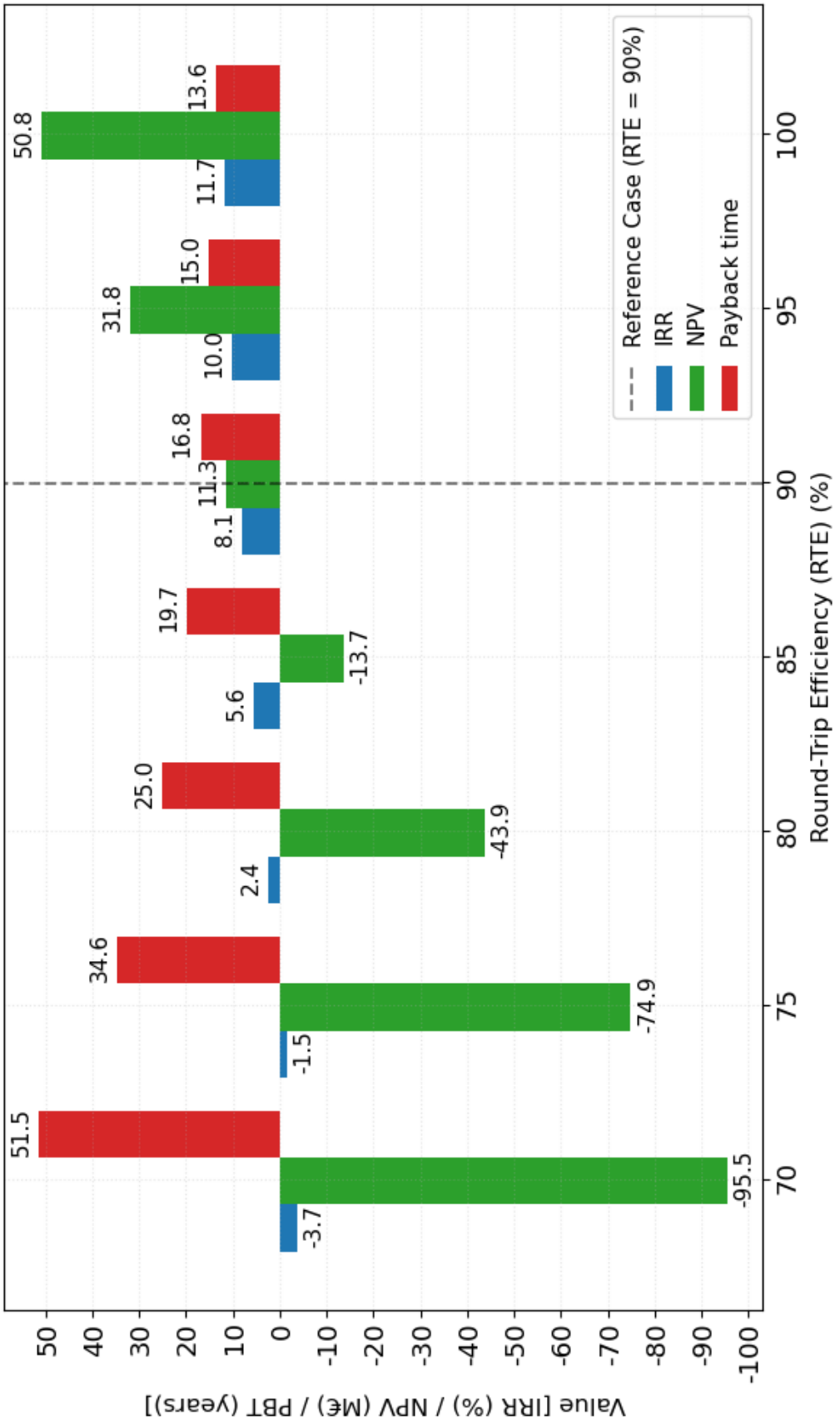

Figure 4.9: Comparison of round-trip efficiency impact on the net present value, internal rate of return and payback time

Chapter 5

Discussion

This chapter discusses the results from the techno-economic optimization model, focusing on their implications for BESS-integrated offshore wind systems in the German day-ahead market.

5.1 Optimal system Configuration and economic viability

The results show that integrating a battery energy storage system (BESS) with offshore wind farms can be economically viable under specific conditions. In the reference case, which uses a 5-hour BESS storage duration (125 MW/625 MWh), the project achieves an IRR of 8.1%, exceeding the 7% discount rate threshold for profitability. This shows that the project is profitable, although the returns are modest and require careful optimization of system parameters. The 5-hour configuration performs better than shorter durations by capturing extended price spreads in the day-ahead market, which suggests that storage durations of 4 to 5 hours are best suited for the studied case.

With a cycling frequency of roughly 0.8 cycles per day, the system uses the battery efficiently, and supports an 18-year lifetime. However, the payback period of 16.8 years is relatively extended, resulting in a short profitability window of approximately 1.2 years. This financial profile may appeal to investors who prioritize long-term returns and are comfortable with prolonged payback periods.

A comparison of onshore and offshore BESS placement highlights significant cost differences. Offshore deployment is not viable under current conditions due to the 50% CAPEX premium assumption, resulting in negative NPV. Offshore BESS deployment does offer advantages, such as greater space availability compared to land-constrained onshore sites, but these benefits are outweighed by their higher deployment costs.

For developers, the findings highlight the importance of strategic timing. Since profitability is marginal, project success depends on cost reductions, selecting the right battery configurations (Energy and power capacities, storage duration, C-rate, etc.), and favorable market conditions. Long payback periods emphasize the need for patient capital and supportive financing. In addition, the sensitivity to CAPEX and

DAM prices means projects require risk assessment and possibly other revenue sources beyond day-ahead arbitrage to enhance economics.

5.2 Critical sensitivity factors

The sensitivity analysis identifies CAPEX and day-ahead market prices as the primary drivers of project viability. A 20% reduction in CAPEX increases NPV by nearly five times compared to the base case, while a 20% increase renders the project unprofitable. This indicates that predicted future battery cost reductions could significantly improve economic performance.

Market price volatility represents a critical determinant of the BESS's economic performance, as demonstrated by the sensitivity analysis. A 20% price increase raises NPV by nearly 6 times, reflecting the BESS's ability to capture larger price spreads. Conversely, a 20% reduction in prices results in a negative NPV and an IRR of 3.42%, rendering the project unprofitable. Germany's ongoing energy transition, characterized by rapid expansion of renewable generation, introduces significant uncertainty in this regard. While near-term market dynamics, driven by renewable intermittency and grid constraints, may sustain price volatility, the long-term increase in zero-marginal-cost generation is expected to compress price spreads [105]. This dual potential for volatility, either boosting or limiting arbitrage, poses a key risk to project feasibility, underscoring diversified revenue strategies to enhance viability.

Round-trip efficiency (RTE) also has a strong influence on profitability. Improving RTE from 85% to 95% increases NPV by roughly three times, emphasizing the value of high-efficiency battery technologies. By contrast, OPEX variations have only a minor impact, since they account for about 1.5% of CAPEX annually, although efficient operations can still support long-term returns.

The battery degradation in the optimization ensures that results reflect realistic operating conditions. Considering battery degradation reduces NPV by about 65% compared to scenarios where it is ignored, showing how excluding it leads to overly optimistic projections. The reference case's average 3.23% annual degradation rate reflects real life operation. More aggressive cycling could increase revenues but accelerate degradation, shortening battery life and reducing long-term profitability.

5.3 Limitations and assumptions

This study is subject to several limitations. First, the model focuses solely on the day-ahead market, excluding potential revenue streams from intraday and ancillary services markets, such as Frequency Containment Reserve (FCR) and Manual Frequency Restoration Reserve (mFRR), which could significantly improve the economic viability of the battery energy storage system.

The wind power model also simplifies wake loss calculations by applying a fixed percentage without accounting for wind farm positioning or turbine spacing, and it disregards wind direction variability. These assumptions may lead to an overestimation of energy yield.

The degradation model estimates cycle aging from total throughput using a polynomial function and approximates calendar aging with a fixed percentage. However, it may not accurately reflect reality, as this method does not capture more complex factors like temperature effects or non-linear aging behavior.

The analysis also assumes perfect forecasting by applying historical data retrospectively. In practice, forecast errors could reduce arbitrage opportunities, meaning actual performance may be lower. Also, the simulation relies on a single year of day-ahead market price data applied across the entire project horizon, which may not capture future price trends or market changes.

In addition, the model treats round-trip efficiency (RTE) as constant throughout the project lifetime, although efficiency is likely to decline as the battery ages.

Chapter 6

Conclusion and future work

6.1 Conclusion

The aim of this thesis was to evaluate the economic feasibility of lithium-ion battery energy storage systems (BESS) for offshore wind farms, focusing on energy arbitrage in the German day-ahead market.

To this end, an energy management system (EMS) was implemented using mixed-integer linear programming (MILP) and model predictive control (MPC) to optimize charging and discharging cycles, for both onshore and offshore BESS placement in a wind farm cluster. Annual revenues were then evaluated against lifecycle costs to determine overall viability. The model was applied to a case study of the BorWin2 offshore grid connection platform, simulating wind power production based on historical wind speed data and turbine power curves. The EMS optimized operations for a fixed 125 MW BESS power rating with varying energy capacities, while explicitly accounting for battery degradation to balance revenue maximization and system longevity.

The results demonstrate that integrating BESS with offshore wind farms can be economically viable under specific conditions, although profitability margins remain modest. In the representative 2023 scenario, the optimal onshore configuration with a five-hour storage duration (625 MWh) achieved an internal rate of return (IRR) of 8.1%, surpassing the assumed 7% discount rate and yielding a positive net present value (NPV) of 11.29 M€, with a payback time (PBT) of 16.8 years. Nevertheless, the long payback period suggests that such projects require patient capital and are most suitable for investors comfortable with extended return horizons. Conversely, offshore BESS deployment remains economically unviable due to a 50% CAPEX premium assumed, resulting in negative returns (IRR -0.30%, NPV -98.48 M€).

Sensitivity analysis highlights that project viability is highly dependent on CAPEX and day-ahead market price volatility. The latter is particularly relevant in the context of Germany's ongoing energy transition, where increasing renewable penetration may reduce price spreads, thereby constraining arbitrage opportunities. The analysis further demonstrates that neglecting battery degradation leads to overly optimistic projections, with NPV overestimated by approximately 65%. This underscores the critical importance of realistic degradation modeling. Round-trip efficiency was also

identified as a major performance driver: improving efficiency from 85% to 95% could potentially triple NPV, emphasizing the value of advanced, high-efficiency battery technologies. By contrast, variations in operational expenditure exhibited minimal impact, given their relatively small share

These findings are constrained by the focus on day-ahead market operations only, where multi-market participation including intraday and ancillary services could significantly enhance viability. The study's limitations include simplified wind power modeling, constant efficiency assumptions, perfect forecasting scenarios, and reliance on single-year price data extrapolated across the project lifetime, all of which may lead to performance overestimation.

In summary, while BESS integration with offshore wind farms demonstrates economic potential under current market conditions, profitability remains marginal and highly sensitive to cost structures and market dynamics. Future success will depend on strategic project timing, and diversification of revenue streams. For developers, this implies a need of comprehensive risk assessment, and adaptive strategies to capture existing opportunities while preparing for evolving market conditions shaped by the continued expansion of renewable generation.

6.2 Future work

Future research should address several areas to enhance the practical applicability and economic viability of BESS-integrated offshore wind systems.

One important direction is to extend the analysis beyond the day-ahead market. For instance, BESS could participate in intraday, balancing, and ancillary services markets in addition to day-ahead trading. By stacking revenues across multiple markets, this approach may enhance profitability and provide a more complete assessment of the economic potential of storage integration.

Also, future studies should consider how operating conditions, such as temperature variations, depth of discharge and non-linear ageing dynamics, affect the battery degradation model. Such refinements would yield more accurate lifetime predictions of the BESS.

In addition, modelling detailed wind farm power production that incorporate site-specific turbine layouts, wake interactions, wind direction variability, and atmospheric conditions would enable more realistic energy yield estimates and improve system sizing accuracy.

Finally, exploring alternative energy storage technologies, such as flow batteries, compressed air energy storage, or other emerging solutions, could identify options that offer improved cost-effectiveness, durability, or technical suitability for offshore wind storage applications.

Bibliography

[1] European Commission, "A roadmap for moving to a competitive low-carbon economy in 2050," 2011. [Online]; Available: https://eur-lex.europa.eu/LexUriServ/LexUriServ.do?uri=COM:2011:0112:FIN:EN:PDF. Accessed: 2025-06-17.

[2] Destatis – Federal Statistical Office of Germany, "Production of energy," 2024. [Online]; Available: https://www.destatis.de/EN/Themes/Economic-Sectors-Enterprises/Energy/Production/_node.html. Accessed: 2025-06-17.

[3] ICLG – International Comparative Legal Guides, "Renewable energy laws and regulations – germany 2025," 2025. [Online]; Available: https://iclg.com/practice-areas/renewable-energy-laws-and-regulations/germany. Accessed: 2025-06-17.

[4] Bundesverband WindEnergie e.V., "Status of offshore wind energy development in Germany – year 2024," Feb. 2025. [Online]; Available: Bundesverband WindEnergie 2024 status of offshore wind energy development in Germany. Accessed: 2025-06-17.

[5] Federal Ministry for Economic Affairs and Climate Action (BMWK), "Climate action in figures – Germany's current emission trends and climate action measures, 2022 edition," July 2022. [Online]; Available: https://www.bmwk.de/Redaktion/EN/Publikationen/Klimaschutz/climate-action-in-figures.pdf. Accessed: 2025-06-18.

[6] Bundesverband WindEnergie e.V., "Status of offshore wind energy development in Germany – first half of 2025," February 2025. [Online]; Available: Bundesverband WindEnergie first half 2025 status of offshore wind energy development in Germany. Accessed: 2025-07-22.

[7] F. M. B. Aldakar, "Energy storage technologies and their role in grid stability," *International Journal of Enhanced Research in Science, Technology & Engineering*, vol. 13, no. 11, p. 94, 2024.

[8] T. Chen, Y. Jin, H. Lv, A. Yang, M. Liu, B. Chen, Y. Xie, and Q. Chen, "Applications of lithium-ion batteries in grid-scale energy storage systems," *Transactions of Tianjin University*, vol. 26, pp. 208–217, 2020.

[9] Fraunhofer Institute for Solar Energy Systems (Fraunhofer ISE), "German net power generation in 2024: Electricity mix cleaner than ever," 2025. [Online]; Available: Fraunhofer ISE Press Release. Accessed: 2025-06-17.

[10] F. A. S. Maldonado, "Techno-economic assessment of lithium ion batteries for utility-scale purpose in the Italian market," master's thesis in management engineering, Politecnico di Milano, Milan, Italy, 2023.

[11] M. Bilousova, A. Motornenko, and F. Hofmann, "Automating storage arbitrage in German electricity market," in *Proceedings of the International Renewable Energy Storage Conference (IRES 2022)*, p. 63–75, Atlantis Press International BV, 2023.

[12] R. B. C. Anto, "Optimization of solar and wind power generation systems with energy storage," master's thesis, Aalto University, 2023.

[13] M. Spiller, G. Rancilio, F. Bovera, G. Gorni, S. Mandelli, F. Bresciani, and M. Merlo, "A model-aware comprehensive tool for battery energy storage system sizing," *Energies*, vol. 16, p. 6546, Sept. 2023.

[14] W. Tong, ed., *Wind Power Generation and Wind Turbine Design*. WIT Transactions on State-of-the-art in Science and Engineering, Vol. 44, Southampton, UK: WIT Press, 2010.

[15] C. Paik, Y. Chung, and Y. J. Kim, "Power curve modeling of wind turbines through clustering-based outlier elimination," *Applied System Innovation*, vol. 6, no. 2, p. 41, 2023.

[16] S. Rehman, M. Alam, L. M. Alhems, and M. M. Rafique, "Horizontal axis wind turbine blade design methodologies for efficiency enhancement—a review," *Energies*, vol. 11, no. 3, p. 506, 2018.

[17] A. Gosk, "Model predictive control of a wind turbine," master's thesis, Technical University of Denmark, Lyngby, Denmark, 2011. IMM-M.Sc-2011-63, ISSN 0909-3192.

[18] S. Shokrzadeh, M. Jafari Jozani, and E. Bibeau, "Wind turbine power curve modeling using advanced parametric and nonparametric methods," *IEEE Transactions on Sustainable Energy*, vol. 5, no. 4, pp. 1262–1269, 2014.

[19] R. Kurt, R. Christoph, B. Stefan, J. Malte, S. Malte, P. Sebastian, and D. Michael, "The importance of offshore wind energy in the energy sector and for the German energiewende," executive summary, Fraunhofer Institute for Wind Energy and Energy System Technology IWES, 2013.

[20] D. Hansson and W. Niilekselä, "Assessing offshore wind system integration: Comparative analysis of floating photovoltaics, oscillating surge wave converters, and battery energy storage systems," master's thesis, Lund University, Sweden, 2023.

[21] TenneT, "Borwin2," 2025. [Online]; Available: https://www.tennet.eu/de-en/projects/borwin2. Accessed: 2025-08-21.

[22] L. Maluck, "Umweltfreundlicher Notstrom auf hoher See," may 2021. [Online]; Available: https://www.mtu-solutions.com/eu/de/stories/energie/gas-generatoren/green-emergency-power-on-the-high-seas.html. Accessed: 2025-07-22.

[23] International Energy Agency, "Offshore wind outlook 2019," world energy outlook special report, International Energy Agency, 2019. [Online]; Available: https://www.iea.org/reports/offshore-wind-outlook-2019. Accessed: 2025-09-16.

[24] Luxwisp, "Pros and cons of offshore wind farms," 2025. [Online]; Available: https://www.luxwisp.com/pros-and-cons-of-offshore-wind-farms/. Accessed: 2025-07-26.

[25] World Forum Offshore Wind, "Global offshore wind report 2024," April 2025. [Online]; Available: https://wfo-global.org/wp-content/uploads/2025/04/WFO_Global-Offshore-Wind-Report-2024_final.pdf. Accessed: 2025-07-22.

[26] WindEurope, "Wind energy in Europe: 2024 statistics and the outlook for 2025–2030," February 2025. [Online]; Available: https://windeurope.org/data/products/wind-energy-in-europe-2024-statistics-and-the-outlook-for-2025-2030. Accessed: 2025-07-22.

[27] S. C. Warder and M. D. Piggott, "The future of offshore wind power production: Wake and climate impacts," *Applied Energy*, vol. 380, p. 124956, Feb. 2025.

[28] M. M. Rahman, A. O. Oni, E. Gemechu, and A. Kumar, "Assessment of energy storage technologies: A review," *Energy Conversion and Management*, vol. 223, p. 113295, Nov. 2020.

[29] H. Bijl, "Techno-economic analysis of energy storage systems for offshore wind farms," master's thesis, University of Groningen, Faculty of Science and Engineering, Groningen, Netherlands, Apr. 2019.

[30] E. Enasel and G. Dumitrascu, "Storage solutions for renewable energy: A review," *Energy Nexus*, vol. 17, p. 100391, Mar. 2025.

[31] G. G. Njema, R. B. O. Ouma, and J. K. Kibet, "A review on the recent advances in battery development and energy storage technologies," *Journal of Renewable Energy*, vol. 2024, p. 1–35, May 2024.

[32] N. Nitta, F. Wu, J. T. Lee, and G. Yushin, "Li-ion battery materials: present and future," *Materials Today*, vol. 18, p. 252–264, June 2015.

[33] A. A. Nkembi, M. Simonazzi, D. Santoro, P. Cova, and N. Delmonte, "Comprehensive review of energy storage systems characteristics and models for automotive applications," *Batteries*, vol. 10, p. 88, Mar. 2024.

[34] A. Solovev and A. Petrova, "Efficient energy management and energy saving with a BESS (battery energy storage system)," Aug. 2021. [Online]; Available: `https://www.integrasources.com/blog/energy-management-and-energy-saving-bess`. Accessed: 2025-07-29.

[35] H. Kang, S. Jung, M. Lee, and T. Hong, "How to better share energy towards a carbon-neutral city? a review on application strategies of battery energy storage system in city," *Renewable and Sustainable Energy Reviews*, vol. 157, p. 112113, Apr. 2022.

[36] L. Grimm, S. Binz, J. Ahn, M. Hummel, and J. Narita, "Battery energy storage systems in Korea and Germany: Current status and prospects," tech. rep., adelphi consult GmbH, Berlin, June 2025. Published by the Korean-German Energy Partnership Team.

[37] National Renewable Energy Laboratory (NREL), "Grid-scale battery storage frequently asked questions," tech. rep., National Renewable Energy Laboratory, 2019. [Online]; Available: `https://docs.nrel.gov/docs/fy19osti/74426.pdf`. Accessed: 2025-07-30.

[38] O. Schmidt and I. Staffell, *Monetizing Energy Storage: A Toolkit to Assess Future Cost and Value*. Oxford, UK: Oxford University Press, Sept. 2023.

[39] Terna, "Study on reference technologies for electricity storage," 2023. [Online]; Available: `https://download.terna.it/terna/Study_on_electricity_storage_reference_technologies_8db99b53d98c32b.pdf`. Accessed: 2025-10-08.

[40] G. Yüksek and A. Alkaya, "Effect of the depth of discharge and C-rate on battery degradation and cycle life," in *Proceedings of the 14th International Conference on Electrical and Electronics Engineering (ELECO 2023)*, p. 212, IEEE, 2023.

[41] Battery Council International, *BCI Acronyms and Glossary of Common Battery Terms*. Battery Council International, Washington, D.C., Jan. 2025. [Online]; Available: `https://batterycouncil.org/wp-content/uploads/2024/12/BCIS-101-BCI-Glossary-of-Common-Battery-Terms-012425.pdf`. Accessed: 2025-07-30.

[42] K. P. P, R. Sudhakar, R. E, I. A. Basha, Y. Ravi Kishore, and R. Geetha, "Exploring cycle and calendar life in lithium ion batteries with an emphasis on degradation assessment," in *2025 International Conference on Electronics and Renewable Systems (ICEARS)*, p. 275–280, IEEE, Feb. 2025.

[43] M. Jafari, A. Botterud, and A. Sakti, "Estimating revenues from offshore wind-storage systems: The importance of advanced battery models," *Applied Energy*, vol. 276, p. 115417, Oct. 2020.

[44] M. A. Hossain, H. R. Pota, S. Squartini, F. Zaman, and J. M. Guerrero, "Energy scheduling of community microgrid with battery cost using particle swarm optimisation," *Applied Energy*, vol. 254, p. 113723, Nov. 2019.

[45] M. Montalà Palau, M. Cheah Mañé, and O. Gomis-Bellmunt, "Techno-economic optimization for BESS sizing and operation considering degradation and ramp rate limit requirement," *Journal of Energy Storage*, vol. 105, p. 114631, Jan. 2025.

[46] Baldauf, "Trading techniques for European electricity markets," master's thesis degree project, Universitat Politècnica de Catalunya (UPC), Escola Tècnica Superior d'Enginyeria Industrial de Barcelona (ETSEIB), Barcelona, Spain, Apr. 2018.

[47] N. Collath, *Aging-Aware Operation of Lithium-Ion-Based Battery Energy Storage Systems*. Ph.d. dissertation, Technical University of Munich, School of Engineering and Design, Munich, Germany, Mar. 2025.

[48] T. Dobos, M. Bichler, and J. Knörr, "Challenges in finding stable price zones in European electricity markets: Aiming to square the circle?," *Applied Energy*, vol. 382, p. 125315, Mar. 2025.

[49] A. Bader, *Entwicklung eines Verfahrens zur Strompreisvorhersage im kurzfristigen Intraday-Handelszeitraum*. Ph.d. dissertation, RWTH Aachen University, Aachen, Germany, 2017.

[50] C. Koch, "Intraday imbalance optimization: incentives and impact of strategic intraday bidding behavior," *Energy Systems*, vol. 13, p. 409–435, May 2021.

[51] D. E. Hugenholtz, "Batteries and energy arbitrage: A techno-economic analysis of electricity arbitrage opportunities for utility-scale battery energy storage in the netherlands," Master's thesis, Delft University of Technology, Delft, The Netherlands, Aug. 2020.

[52] B. Xiao, "Maximizing energy cost savings: A milp-based energy management system in educational buildings: Case study in stockholm," Master's thesis, KTH Royal Institute of Technology, School of Electrical Engineering and Computer Science (EECS), Stockholm, Sweden, Feb. 2024.

[53] K. Reinders, "Model predictive controller for a battery energy storage system to reshape the energy demand curve of an office: Case study in the netherlands," Master's thesis, Eindhoven University of Technology, Eindhoven, Netherlands, Oct. 2022.

[54] S. P. Englberger, *Optimized energy management for battery energy storage via multi-use and multi-storage operation*. Ph.d. dissertation, Technical University of Munich, School of Engineering and Design, Munich, Germany, March 2022.

[55] A. Grimaldi, F. D. Minuto, A. Perol, S. Casagrande, and A. Lanzini, "Techno-economic optimization of utility-scale battery storage integration with a wind

farm for wholesale energy arbitrage considering wind curtailment and battery degradation," *Journal of Energy Storage*, vol. 112, p. 115500, Mar. 2025.

[56] N. Collath, M. Cornejo, V. Engwerth, H. Hesse, and A. Jossen, "Increasing the lifetime profitability of battery energy storage systems through aging aware operation," *Applied Energy*, vol. 348, p. 121531, Oct. 2023.

[57] A. Grimaldi, F. D. Minuto, J. Brouwer, and A. Lanzini, "Profitability of energy arbitrage net profit for grid-scale battery energy storage considering dynamic efficiency and degradation using a linear, mixed-integer linear, and mixed-integer non-linear optimization approach," *Journal of Energy Storage*, vol. 95, p. 112380, Aug. 2024.

[58] D. Atabay, *Comparison of Optimization Methods for Model Predictive Control: An Application to a Compressed Air Energy Storage System*. Ph.d. dissertation, Technical University of Munich, Department of Electrical and Computer Engineering, Munich, Germany, Apr. 2018.

[59] S. Bergsvik, "Enhancing model predictive control for non-continuous actuators in the oil and gas industry: A mixed integer mpc approach," Master's thesis, Norwegian University of Science and Technology, Faculty of Information Technology and Electrical Engineering, Department of Engineering Cybernetics, Trondheim, Norway, June 2023.

[60] A. Botelho, B. Parreira, P. N. Rosa, and J. M. Lemos, *Predictive Control for Spacecraft Rendezvous*. SpringerBriefs in Applied Sciences and Technology, Cham, Switzerland: Springer, 2021.

[61] A. L. Cedeño, R. López Ahuar, J. Rojas, G. Carvajal, C. Silva, and J. C. Agüero, "Model predictive control for photovoltaic plants with non-ideal energy storage using mixed integer linear programming," *Energies*, vol. 15, p. 6427, Sept. 2022.

[62] A. Wiese, "The mixed-integer program coding cookbook (using Python and Pyomo)," 2024. [Online]; Available: `https://www.math.cit.tum.de/fileadmin/w00ccg/math/personen/discrete_math/Andreas_Wiese/MIP-coding-cookbook.pdf`. Accessed: 2025-08-06.

[63] O. Grothe, F. Kächele, and M. Watermeyer, "Analyzing Europe's biggest offshore wind farms: A data set with 40 years of hourly wind speeds and electricity production," *Energies*, vol. 15, p. 1700, Feb. 2022.

[64] Copernicus Climate Change Service (C3S), "ERA5 hourly data on single levels from 1940 to present," 2024. [Online]; Available: `https://cds.climate.copernicus.eu/datasets/reanalysis-era5-single-levels`. Accessed: 2025-08-09.

[65] Bundesnetzagentur, "SMARD – StromMarktDaten: Electricity market data platform," 2024. [Online]; Available: `https://www.smard.de/home/downloadcenter/download-marktdaten/`. Accessed: 2025-08-09.

[66] The Wind Power, "Siemens SWT-6.0-154," 2018. [Online]; Available: https://www.thewindpower.net/turbine_en_807_siemens_swt-6.0-154.php. Accessed: 2025-08-09.

[67] L. Bauer and S. Matysik, "Vestas V164-8.0," 2025. [Online]; Available: https://en.wind-turbine-models.com/turbines/318-vestas-v164-8.0. Accessed: 2025-08-09.

[68] M. Lydia, S. S. Kumar, A. I. Selvakumar, and G. E. Prem Kumar, "A comprehensive review on wind turbine power curve modeling techniques," *Renewable and Sustainable Energy Reviews*, vol. 30, p. 452–460, Feb. 2014.

[69] V. Sohoni, S. C. Gupta, and R. K. Nema, "A critical review on wind turbine power curve modelling techniques and their applications in wind based energy systems," *Journal of Energy*, vol. 2016, p. 1–18, 2016.

[70] B. Wacker and J. C. Schlüter, "Pipeline for annual averaged wind power output generation prediction of wind turbines based on large wind speed data sets and power curve data," *MethodsX*, vol. 8, p. 101499, 2021.

[71] K. Ma, H. Zhang, X. Gao, X. Wang, H. Nian, and W. Fan, "Research on evaluation method of wind farm wake energy efficiency loss based on scada data analysis," *Sustainability*, vol. 16, p. 1813, Feb. 2024.

[72] J. McMorland, M. Collu, D. McMillan, J. Carroll, and A. Coraddu, "Opportunistic maintenance for offshore wind: A review and proposal of future framework," *Renewable and Sustainable Energy Reviews*, vol. 184, p. 113571, Sept. 2023.

[73] S. Koukoura, M. N. Scheu, and A. Kolios, "Influence of extended potential-to-functional failure intervals through condition monitoring systems on offshore wind turbine availability," *Reliability Engineering amp; System Safety*, vol. 208, p. 107404, Apr. 2021.

[74] U.S. Energy Information Administration, "Assessing hvdc transmission for impacts of non-dispatchable generation," technical report, U.S. Department of Energy, 2018.

[75] M. Ardelean and P. Minnebo, "Hvdc submarine power cables in the world: State-of-the-art knowledge," Science-for-Policy Report OTG Work Package Deliverable, Joint Research Centre, Publications Office of the European Union, 2015.

[76] H. Jaffal, L. Guanetti, G. Rancilio, M. Spiller, F. Bovera, and M. Merlo, "Battery energy storage system performance in providing various electricity market services," *Batteries*, vol. 10, p. 69, Feb. 2024.

[77] K. Shan, S. Wang, and R. Tang, "Direct chiller power limiting for peak demand limiting control in buildings—methodology and on-site validation," *Automation in Construction*, vol. 85, p. 333–343, Jan. 2018.

[78] F. Wankmüller, P. R. Thimmapuram, K. G. Gallagher, and A. Botterud, "Impact of battery degradation on energy arbitrage revenue of grid-level energy storage," *Journal of Energy Storage*, vol. 10, p. 56–66, Apr. 2017.

[79] Y. Wang, Z. Zhou, A. Botterud, K. Zhang, and Q. Ding, "Stochastic coordinated operation of wind and battery energy storage system considering battery degradation," *Journal of Modern Power Systems and Clean Energy*, vol. 4, p. 581–592, Oct. 2016.

[80] P. L. Camuñas García-Miguel, J. Alonso-Martinez, S. Arnaltes Gómez, M. García Plaza, and A. Peña Asensio, "Battery degradation impact on long-term benefits for hybrid farms in overlapping markets," *Batteries*, vol. 9, p. 483, Sept. 2023.

[81] National Renewable Energy Laboratory (NREL), "Utility-scale battery storage (2022 annual technology baseline)," 2022. [Online]; Available: `https://atb.nrel.gov/electricity/2022/utility-scale_battery_storage`. Accessed: 2025-07-12.

[82] Exencell, "BESS costs analysis: Understanding the true costs of battery energy storage systems," Aug. 2024. [Online]; Available: Exencell BESS cost analysis. Accessed: 2025-07-22.

[83] J. Huttunen, "Profitability of lithium battery energy storage system on a solar power plant," master's thesis, Lappeenranta–Lahti University of Technology (LUT), School of Engineering Science, Industrial Engineering and Management, Lappeenranta, Finland, 2023.

[84] P. Jivaganont, P. Limthongkul, and J. Mongkoltanatas, "Profitability of battery energy storage system coupled with photovoltaic at behind-the-meter," *Journal of Energy Storage*, vol. 121, p. 116357, June 2025.

[85] HM Revenue and Customs, "April 2025 HMRC currency exchange monthly rates." [Online]; Available: `https://www.trade-tariff.service.gov.uk/exchange_rates/view/2025-4`. Accessed: 2025-05-06.

[86] S. Orangi, N. B. Manjong, D. P. Clos, L. Usai, O. Stokke Burheim, and A. H. Strømman, "Trajectories for lithium-ion battery cost production: Can metal prices hamper the deployment of lithium-ion batteries?," *Batteries amp; Supercaps*, vol. 6, Oct. 2023.

[87] Aditya, "Techno-economic analysis of utility-scale BESS projects," Master's thesis, KTH Royal Institute of Technology, School of Industrial Engineering and Management, Stockholm, Sweden, 2024.

[88] L. Smajila, S. Trevisan, F. Golzar, K. Vaidya, and R. Guedez, "Comparative analysis of techno-economic and techno-environmental approach to optimal sizing and dispatch of hybrid solar–battery systems," *Energy Conversion and Management: X*, vol. 25, p. 100858, Jan. 2025.

[89] I. Hauer, S. Balischewski, and C. Ziegler, "Design and operation strategy for multi-use application of battery energy storage in wind farms," *Journal of Energy Storage*, vol. 31, p. 101572, Oct. 2020.

[90] J. Arnelo, "Techno-economic optimization of a hybrid wind and battery system: Modelling and assessment of a hybrid power plant in the south of sweden," master's thesis, KTH Royal Institute of Technology, June 2025.

[91] L. Silvestri and M. De Santis, "Renewable-based load shifting system for demand response to enhance energy-economic-environmental performance of industrial enterprises," *Applied Energy*, vol. 358, p. 122562, Mar. 2024.

[92] M. Victoria and C. Gallego-Castillo, "Economics of photovoltaic solar energy," in *Fundamentals of Solar Cells and Photovoltaic Systems Engineering*, p. 429–457, Elsevier, 2025.

[93] Y. Meng, "Economic analysis for centralized battery energy storage system with reused battery from ev in australia," *E3S Web of Conferences*, vol. 300, p. 01003, 2021.

[94] A. Berrada, "Financial and economic modeling of large-scale gravity energy storage system," *Renewable Energy*, vol. 192, p. 405–419, June 2022.

[95] M. H. Hansen and O. C. Handegård, "Historical development and outlook of offshore wind: Dudgeon offshore wind farm case study," master's thesis, Norwegian University of Science and Technology (NTNU), Faculty of Science and Technology, Trondheim, Norway, spring 2022.

[96] J. M. González-Ramírez, Arcos-Vargas, and F. Núñez, "Optimal sizing of hybrid wind-photovoltaic plants: A factorial analysis," *Sustainable Energy Technologies and Assessments*, vol. 57, p. 103155, June 2023.

[97] The Wind Power, "Deutsche Bucht (Germany)," 2025. [Online]; Available: `https://www.thewindpower.net/windfarm_de_10294_deutsche-bucht.php`. Accessed: 2025-09-09.

[98] The Wind Power, "Albatros (Germany)," 2025. [Online]; Available: `https://www.thewindpower.net/windfarm_en_16883_albatros.php`. Accessed: 2025-08-12.

[99] The Wind Power, "Veja Mate (Germany)," 2025. [Online]; Available: `https://www.thewindpower.net/windfarm_en_10353_veja-mate.php`. Accessed: 2025-08-12.

[100] Power Technology, "Deutsche Bucht offshore wind farm, North sea, Germany," 2025. [Online]; Available: `https://www.power-technology.com/projects/deutsche-bucht-offshore-windfarm/`. Accessed: 2025-08-12.

[101] Power Technology, "Albatros offshore wind farm,North sea, Germany," 2025. [Online]; Available: `https://www.power-technology.com/projects/albatros-offshore-wind-farm-north-sea/`. Accessed: 2025-08-12.

[102] Power Technology, "Veja Mate offshore wind farm project, German North sea," 2025. [Online]; Available: `https://www.power-technology.com/projects/veja-mate-offshore-wind-farm-project/`. Accessed: 2025-08-12.

[103] W. Pan and E. Shittu, "Optimizing energy storage capacity for enhanced resilience: The case of offshore wind farms," *Applied Energy*, vol. 378, p. 124718, Jan. 2025.

[104] P. Morthorst and L. Kitzing, "Economics of building and operating offshore wind farms," in *Offshore Wind Farms*, p. 9–27, Elsevier, 2016.

[105] L. Lev and M. Dolmatova, "Impact of high renewable energy penetration on price volatility: A comparative analysis of Denmark and Germany," in *2025 7th International Youth Conference on Radio Electronics, Electrical and Power Engineering (REEPE)*, p. 1–6, IEEE, Apr. 2025.

[106] J. Simpson, G. Hanrahan, E. Loth, G. Koenig, and D. Sadoway, "Liquid metal battery storage in an offshore wind turbine: Concept and economic analysis," *Renewable and Sustainable Energy Reviews*, vol. 149, p. 111387, Oct. 2021.

Appendix A

Wind turbine data and power curves

As discussed in Section 3.5, the case study consists of three offshore wind farms: *Veja Mate* uses Siemens SWT-6.0-154 turbines, *Deutsche Bucht* employs MHI Vestas V164-8.4MW turbines, and *Albatros* operates Siemens SWT-7.0-154 turbines. Power curves for *Veja Mate* were obtained from manufacturer specifications [66]. *Deutsche Bucht* turbine power curves were scaled from MHI Vestas V164-8.0MW wind turbine curves [67] using a scaling factor of 1.05, while the power curves for the wind turbines in *Albatros* were scaled from *Veja Mate* wind turbine curves using a scaling factor of 1.167. The complete power curve data is presented in Table A.1 and visualized in Figure A.1.

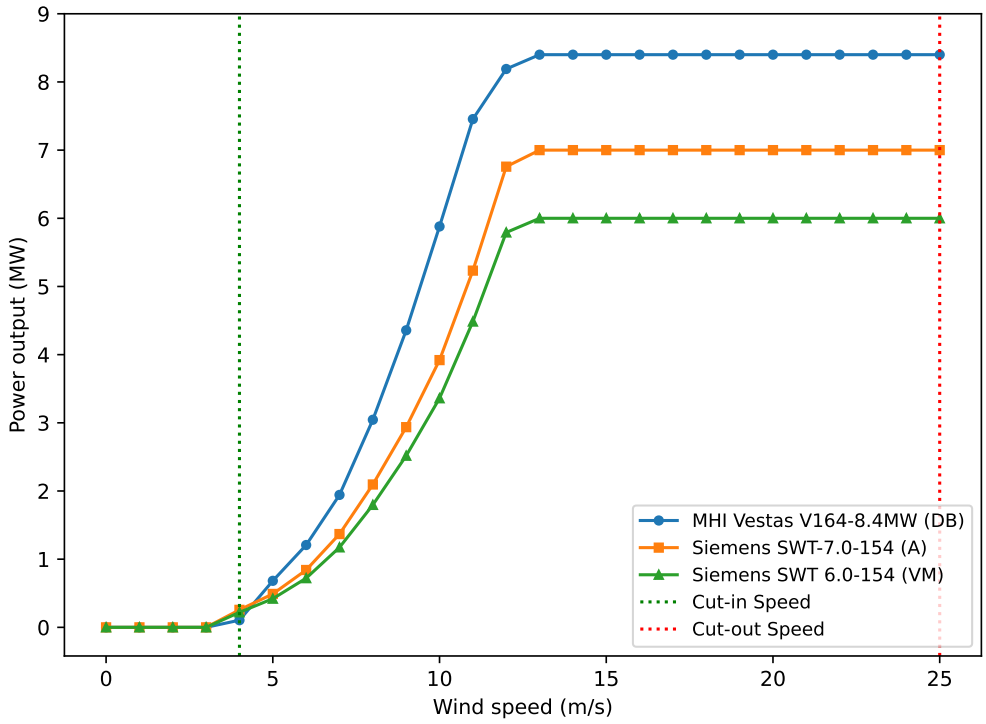

Figure A.1: Power curves of the wind turbine models used in the study

Table A.1: Power curve points for wind turbines used in the study [66, 67]

Wind Speed $[m/s]$	**Deutsche Bucht** V164-8.4MW [kW]	**Albatros** SWT-7.0-154 [kW]	**Veja Mate** SWT-6.0-154 [kW]
1	0	0	0
2	0	0	0
3	0	0	0
4	105	257	220
5	683	490	420
6	1,208	841	721
7	1,943	1,369	1,173
8	3,045	2,095	1,796
9	4,358	2,937	2,517
10	5,880	3,920	3,360
11	7,455	5,233	4,485
12	8,190	6,757	5,792
13	8,400	7,000	6,000
14	8,400	7,000	6,000
15	8,400	7,000	6,000
16	8,400	7,000	6,000
17	8,400	7,000	6,000
18	8,400	7,000	6,000
19	8,400	7,000	6,000
20	8,400	7,000	6,000
21	8,400	7,000	6,000
22	8,400	7,000	6,000
23	8,400	7,000	6,000
24	8,400	7,000	6,000
25	8,400	7,000	6,000

List of Figures

List of Tables

Usage of AI tools

Table A.2: Usage of AI tools

AI tool	**Purpose**
ChatGPT	Translating and paraphrasing text
Grok	Assistance with Python coding and error handling in the code
DeePL	Text translation, improving text structure and grammatical accuracy
Overleaf	PDF editing and compilation